Ilia State University
Institute of Theoretical Physics
Center of Theoretical Astrophysics

Mariam Akhalkatsi

WAVE GENERATION BY TURBULENT CONVECTION

Dissertation Presented in Partial Fulfilment of the Requirements

for the Degree of Doctor of Physics

Supervisor: Professor Giorgi Machabeli

Tbilisi, 2011

Contents

Introduction

Aeroacoustics is concerned with sound generated by aerodynamic forces or motions originating in a flow rather than by the externally applied forces or motions of classical acoustics. Thus, the sounds generated by vibrating violin strings and loudspeakers, i.e. produced by the vibration of solids, fall into the category of classical acoustics, whereas sound generated by the unsteady aerodynamic forces on propellers or by turbulent flows fall into the domain of aeroacoustics.

The airflow may contain fluctuations as a result of instability. At low Reynolds numbers, when viscous forces are larger than inertial forces (laminar flow) these fluctuations give a regular eddy pattern which is responsible for the sound produced by musical wind instruments. At high Reynolds numbers inertial forces are dominant and initial fluctuations result in an irregular turbulent motion (turbulent flow) which is responsible for the roar of the wind and of jet aeroplanes.

Pressure fluctuations occur in an unsteady flow in order to balance the fluctuations in momentum. All real fluids posses both elasticity and inertia. Elasticity causes the fluid to resist compression while inertia causes it to "overshoot" whenever it is displaced. Because of these two properties, pressure (or density) fluctuations propagate outward from their source and, if an observer is present, will subsequently be recognized as sound.

At low Mach numbers the pressure variations in the vicinity of a localized flow are substantially uninfluenced by compressibility and can be determined from the velocity field by solving a Poisson's equation

$$\nabla^2 p = \gamma. \tag{1}$$

Here the source term γ is a known function of the instantaneous velocity.

Moreover, the Biot-Savart law shows that it is possible to treat the velocity field as if it were in turn driven by a prescribed vorticity field. However, Kelvin's theorem of conservation of circulation shows that the vorticity in an inviscid fluid is simply carried along with the flow and, as a consequence, that any initially localized region of vorticity will remain that way for some time to come. Thus, many flows can be envisioned as relatively concentrated regions of vorticity which drive not only the pressure fluctuations in their immediate vicinity but also those at large distances.

The theory of aerodynamic sound is concerned with pressure fluctuations that occur far from the source where the amplitude of the motion is small and the effects of compressibility and finite propagation speed of the disturbances are important. This region is called acoustic field. The pressure (and density) fluctuations are weak in this region and satisfy the acoustic wave equation.

The study of flow-generated acoustic waves began with Gutin's theory of propeller noise, which was developed in 1937. He obtained a theoretical expression for the sound produced by a propeller in static operation as a function of tip speed, number of blades, thrust and torque, and the dimensions of the propeller, which was valid at distances large compared with the propeller diameter.

Lighthill (1952, 1954) developed a theory for the sound radiated into free space and thus he neglected neighboring resonators and all effects of reflection, diffraction, absorbtion or scattering by solid boundaries. Ignoring the influence of boundaries on the production of sound as opposed to the production of vorticity reduces the aerodynamic sound problem to the study of mechanisms that convert kinetic energy of rotational motions into acoustic waves involving longitudinal vibrations of fluid particles.

Due to the non-linearity of the governing equations it is very difficult to predict the sound production by fluid flows. This occurs typically for flows with high Reynolds numbers, for which non-linear inertial terms in the equation of

motion are much larger than the viscous terms. Lighthill introduced the idea of calculating the far-field sound generated by unsteady flow with an acoustic analogy to deal with the problem of jet noise. The Lighthill's idea provides an approximation by assuming that the source term is in some sense known or that it can at least be modeled in an approximate fashion. In the lighthill's analogy, the fully nonlinear problem is taken to be analogous to the problem of sound propagating in a linear acoustic medium at rest subject to an external forcing that represents the turbulent source. Lighthill reformulated the Navier-Stokes equation into an exact, inhomogeneous wave equation whose source terms are important only within the turbulent (vortical) region. Sound is expected to be such a very small component of the whole motion that, once generated, its back-reaction on the source region may then be determined by neglecting the production and propagation of the sound.

There are two principal source types in free nonsaturated vortical flows: a quadrupole, whose strength is determined by the unsteady Reynolds stress; a dipole, which is important when mean mass density variations occur within the source region. Proudman (1952) derived an equation for the radiated acoustic power per unit mass of the quadrupole source:

$$N \sim M^5, \tag{2}$$

where M is the turbulent Mach number. In Proudman's (1952) analysis, the equation for acoustic power was derived assuming Gaussian statistics with normal joint probability distributions for the turbulent velocities an their first two time derivatives. Lighthill pointed out that his equations implied that there was an exact analogy between the density fluctuations in any real flow and those produced by a quadrupole source in an ideal (non-moving) acoustic medium.

Lighthill's acoustic analogy would be inappropriate if the Mach number is large enough for compressibility to be important in the source flow, when the

source flow is coupled to a resonator, such as an organ pipe, when solid boundaries or when bubbles are present in the case of liquids. His ideas were subsequently extended by Curle (1955), Powell (1960), and Ffowcs Williams and Hall (1970) to include the effects of solid boundaries. These extensions include Gutin's (1948) analysis for propeller noise and, in fact, provide a complete theory of aerodynamically generated sound that can be used to predict blading noise as well as jet noise.

While Lighthill's strategy turned out to be remarkably successful in predicting the gross features of the sound radiation from turbulent air jets, engine manufacturers needed a much more sensitive tool with the capability of predicting how even relatively small changes in the flow would affect the radiated sound. This resulted in a number of attempts to improve the Lighthill approach. Early efforts were focused on accounting for mean flow interaction effects. Phillips (1960), Lilley (1974), and many others rearranged the Navier-Stokes equations into the form of an inhomogeneous convective or moving-medium wave equation rather than the inhomogeneous stationary-medium wave equation originally proposed by Lighthill. But these methods appeared to be incapable of predicting the changes in the sound field that occur when noise suppression devices are deployed and therefore couldn't be used to evaluate the acoustic performance of these devices.

Goldstein (2002) rewrote the Navier-Stokes equations into the general set of linearized inhomogeneous Euler equations (in convective form) but with modified dependent variables. The source terms are exactly the same as those that would result from externally imposed shear-stress and energy-flux perturbations and the equations are therefore exactly the same as the Navier-Stokes equations, but with the viscous stress perturbation replaced by an appropriate Reynolds stress and the heat flux perturbation replaced by an appropriate enthalpy flux. The "basic flow" about which the equations are linearized can be any solution to a very general class of inhomogeneous Navier-stokes equa-

tions with arbitrarily specified source strengths. His method put the classical approaches to the jet noise problem on a more rational basis and also extended in new directions. The rewritten Navier-Stokes equations remained nonlinear, but the nonlinearity was effectively contained in the generalized Reynold stresses and enthalpy flux - which also contained contributions from the base-flow sources.

The acoustic-analogy-type approaches and their extensions roughly correspond to treating the generalized stresses and enthalpy flux as known source terms that can be estimated or modeled. This doesn't imply that acoustic analogy equations can provide an unambiguous identification of sources, except for the generalized incompressible flows. These equations are only useful when the "base flow" is reasonably close to the actual fluid motion and, in most cases, can only serve as a guide for identifying and ultimately modeling the apparent sources of sound. Since the sound is just a by-product of all the processes occurring in the flow, it is highly unlikely that "true" sound sources can be identified in any realistic turbulent motion.

Validation of Lighthill's acoustic analogy for studding the sound generation by turbulent flows has been shown by various experiments and numerical simulations (Whitmire and Sarkar 2000; Seror *et al.* 2001; Freund 2003; Panickar *et al.* 2005 and references therein), that are based on combined analytical-modeling method.

The most obvious approach to obtain meaningful predictions of the far field sound radiated by turbulence would be to use large-scale numerical simulation, i.e. DNS (direct numerical simulation). The number of mesh points needed to fully resolve any turbulent flow is proportional to the Reynolds number Re based on the characteristic length scale of the turbulent eddies raised to the nine-fourths power. But since typically Re is of the order of 10^5 to 10^7, this means that 10^{12} to 10^{15} grid points would be needed to resolve all of the relevant length scales. This implies that computing the far filed sound by DNS on a

very large computational domain which includes both the turbulent source and the acoustic far field is unfortunately very expensive and problematic for even relatively simple flows.

An alternative strategy is to calculate the sound using a hybrid approach in which the turbulence is computed using a method such as DNS or LES (large eddy simulation), and the far field sound is calculated using an acoustic analogy. In various studies this method was used to calculate the sound from turbulence and compare acoustic-analogy predictions with theoretical and experimental results. Sarkar and Hussaini (1993) computed the sound from decaying isotropic turbulence using a hybrid DNS/Lighthill acoustic-analogy approach. Witkowska *et al.* (1995) also computed the sound from isotropic turbulence for forced and unforced cases using both DNS and LES to evaluate the turbulent source in the Lighthill acoustic analogy. Lilley (1994) derived an alternative analytical method of determining the radiated acoustic power per unit mass of the Lighthill's quadrupole source and evaluated his analytical results using statistics of the Lighthill source obtained from the DNS databases of Sarkar and Hussaini (1993) and Dubois (1993). These studies show that the hybrid acoustic-analogy method can be used to compute the acoustic source and obtain sound radiated by isotropic turbulence.

Validation of various forms of the acoustic analogy for different flow configurations have been performed by comparing the sound calculated from direct computations or exact analytical solutions with acoustic-analogy predictions. Mitchell *et al.* (1992) and Colonius *et al.* (1994) studied the sound radiated by compressible co-rotating vortex pair and the scattering of sound waves from a compressible viscous vortex, respectively. Colonius *et al.* (1995) validate the Lilley acoustic analogy for a forced, two-dimensional, compressible shear layer by comparing DNS results with acoustic-analogy predictions. Mitchell *et al.* (1995) validate the Lighthill acoustic analogy by comparison with DNS results for axisymmetric, nonturbulent subsonic and supersonic jets. In these

studies the emphasis was to investigate the sound from large coherent structures rather than the effects of smaller turbulence scales on the radiated sound. Bastim *et al.* (1995) calculated the sound from a subsonic turbulent plain jet using the hybrid approach. Freund (1999) performed a DNS of a jet with Mach number equal to 0.9 and Reynolds number equal to 3600 and analyzed the acoustic sources in the jet. Whitmire and Sarkar (2000) computed sound from a turbulent flow using DNS and compared their results with acoustic-analogy predictions. They considered a three-dimensional region of forced turbulent flow with a small turbulent Mach number so that the source is spatially compact (i.e. the turbulence integral scale is much smaller than the acoustic wavelength). Seror *et al.* (2001) studied the problem of the estimation of the noise by forced isotropic turbulence using hybrid LES/Lighthill analogy approach. Freund (2003) computed turbulent statistics that are relevant to jet noise modeling using a previously validated simulation database of a cold jet with Mach number $M = 0.9$. Panickar *et al.* (2005) examined instability mode switching in various supersonic jet configurations that involve resonant acoustics (situations where flow instabilities are enhanced by feedback).

All these studies verified the ability of the Lighthill acoustic analogy to predict sound generated by a three-dimensional turbulent source containing many length and time scales.

0.1 Wave generation by turbulent convection. Solar p-Modes. Stellar and planetary atmospheres

Lighthill's method of calculating the aerodynamic emission of sound waves in a homogeneous medium was extended by Stein (1967) to calculate the acoustic and gravity-wave emission by turbulent motions in a stratified atmosphere. In the solar convective region the characteristic size of turbulent eddies is considered to be comparable to the scale height of the stratification produced by gravity. In a stratified environment gravity as well as pressure acts as a restor-

ing force for fluid oscillations, and two types of waves - acoustic and gravity - occur, depending on the dominant restoring force. Stein's analysis showed, that the stratification cuts off the acoustic radiation at low Mach numbers and for typical parameters of the solar convective region gravity-wave emission is much more efficient than acoustic.

Goldreich and Kumar (1990) studied acoustic and gravity wave generation by turbulent convection in a plane parallel, stratified atmosphere that consist of two semi-infinite layers, the lower being adiabatic and polytropic and the upper being isothermal. They estimated efficiencies for the conversion of the convective energy flux into both trapped and propagating waves and calculated the total emissivities for the different wave types. Their theoretical results obtained for the amplitudes and linewidths of the solar p-Modes match the observational ones in the upper part of the solar convection zone. This agreement supports the hypothesis that the solar p-Modes are stochastically excited by turbulent convection.

0.2   The role of waves in the heating of solar chromosphere

The mechanism of chromospheric heating in the Sun has been an important topic of research for many years since the observations of line and continuum emissions by non-active solar surface indicated that chromospheric temperatures are around 6000-7000 K, much higher than those that can be expected for a plasma in radiative equilibrium.

Several potential chromospheric heating mechanisms have been proposed over the years. Most of them are based on observed correlation between the UV intensity distribution with magnetic fields, i.e. the relationship between chromospheric heating and magnetic fields.

Carlsson and Stain (1992) analyzed the idea proposed by Biermann (1946) and Schwarzschild (1948), that the quiet-Sun chromospheric regions are heated

by transient acoustic waves generated in the convective zone. However, measurements of the acoustic energy flux are not consistent with the amount of the energy needed for the heating of the whole chromosphere (Fossum and Carlsson 2005).

Impulsive nano-flares related to magnetic reconnection events (Parker 1988; Sturrock 1999) also appeared not to be sufficiently frequent and energetic to account for the persistent UV emission and chromospheric heating (Aschwanden *et al.* 2000, Carlsson 2007).

As it has been shown recently, the magnetoacoustic waves generated locally, inside or in the vicinity of the magnetic flux tubes (Hasan and van Ballegooijen 2008) can be responsible for heating the quiet-Sun chromosphere. Erdelyi and James (2004) suggested that random Alfven waves can initiate ion-neutral collisions and the consequent heating of the upper chromosphere. This mechanism also can explain the formation of spicules.

An alternative mechanism for chromospheric heating is the resistive dissipation of electric currents (Rabin and Moore 1984; Goodman 2004). However, recent studies (Socas-Navarro 2007) have shown, that resistive current dissipation contributes to heating the sunspot chromosphere, but it is not the dominant factor.

Recent studies (Liperovsky *et al.* 2000; Fontenla 2005; Fontenla *et al.* 2008) suggested that the Farley-Buneman (Farley 1963; Buneman 1963) plasma instability, which can be triggered by the cross-field motions of the neutral component of the partially ionized gas and driven by convective motions of neutral atoms, creates plasma irregularities at heights where the electrons are strongly magnetized and can be responsible for chromospheric heating in the Sun and other cool stars of solar type that have a partially ionized chromosphere. However, Gogoberidze *et al.* (2009) showed that even though the Farley-Buneman instability can sporadically appear in the chromosphere, it cannot be responsible for quasi-steady chromospheric heating at global length scales.
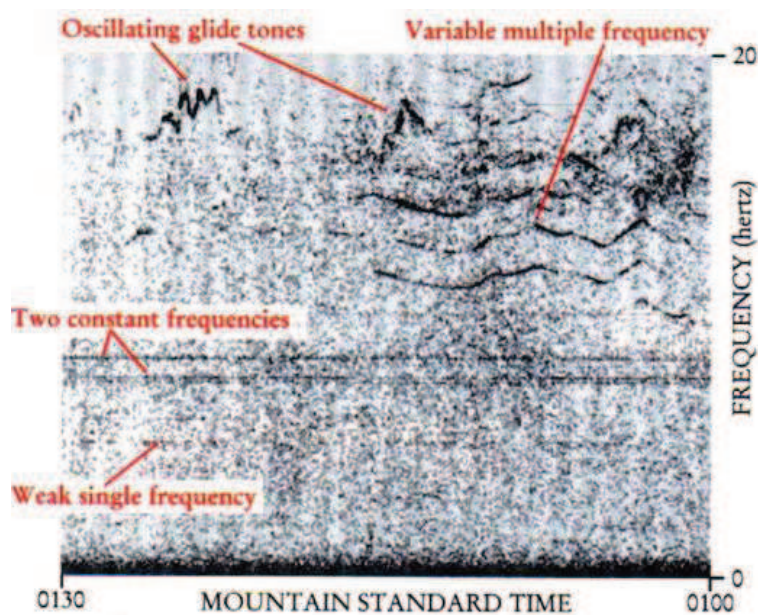
Figure 1: Sonogram of atmospheric infrasound between 1 and 20 Hz, recorded over a 30 min interval at Boulder, Colorado.

Summarizing, although several promising mechanisms of chromospheric heating have been proposed, currently none of them can satisfactorily fit all the observational data. As a consequence, explanation of the chromospheric heating remains one of the most challenging unsolved problems in solar physics.

Because the solar chromosphere is turbulent (Fontenla *et al.* 2008), wave generation by turbulence is natural ingredient of the chromospheric dynamics and can have important contribution to the chromospheric as well as coronal heating.

0.3   Atmospheric infrasound

Atmospheric infrasound was unknown and unheard until the early 1950s of the last century when global infrasonic monitoring network was set to detect, locate and classify nuclear explosions at global distances. This era ended with the evolution of a satellite-based nuclear detection system and since the 1970s, the science of atmospheric infrasound has focused on understanding the origin and structure of natural infrasound. As the example of the richness of

13
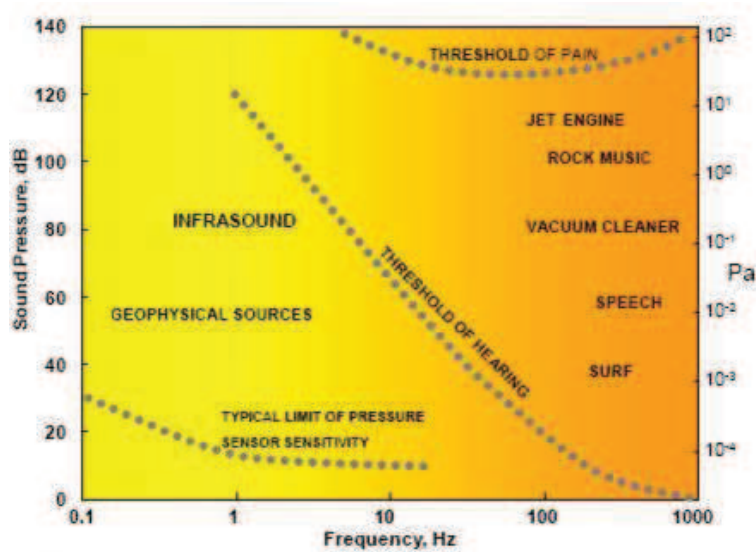
Figure 2: Sound pressure amplitude as a function of frequency compared with the threshold of human hearing at lower frequencies.

the near-infrasound environment, Figure 1 from Bedard and Georges (2000) is a half-hour spectrogram of infrasonic signals between 1 and 20 Hz. Figure 2 from Bedard and Georges (2000) shows the frequency and amplitude ranges of sounds familiar to us. Examples of atmospheric infrasound sources include: avalanches; meteors; ocean waves; severe-weather systems; tornadoes; earthquakes; volcanoes; atmospheric turbulence. Infrasound signals from these sources have different frequency ranges and durations. Most of them are already well identified.

One of the most interesting and useful properties of infrasound is that it travels without significant absorption over global distances. 1 Hz signal is detectable on the distance of about 3000 km from the source. The temperature and wind structure of the atmosphere acts as a waveguide trapping much of the acoustic energy (Georges and Beasley 1977). Some waves emitted from the source escape and travel upward to great heights in the ionosphere where they dissipate, while other sound rays are trapped, bounced back and channeled over long distances.

It has been known for a long time that strong convective storms, such as
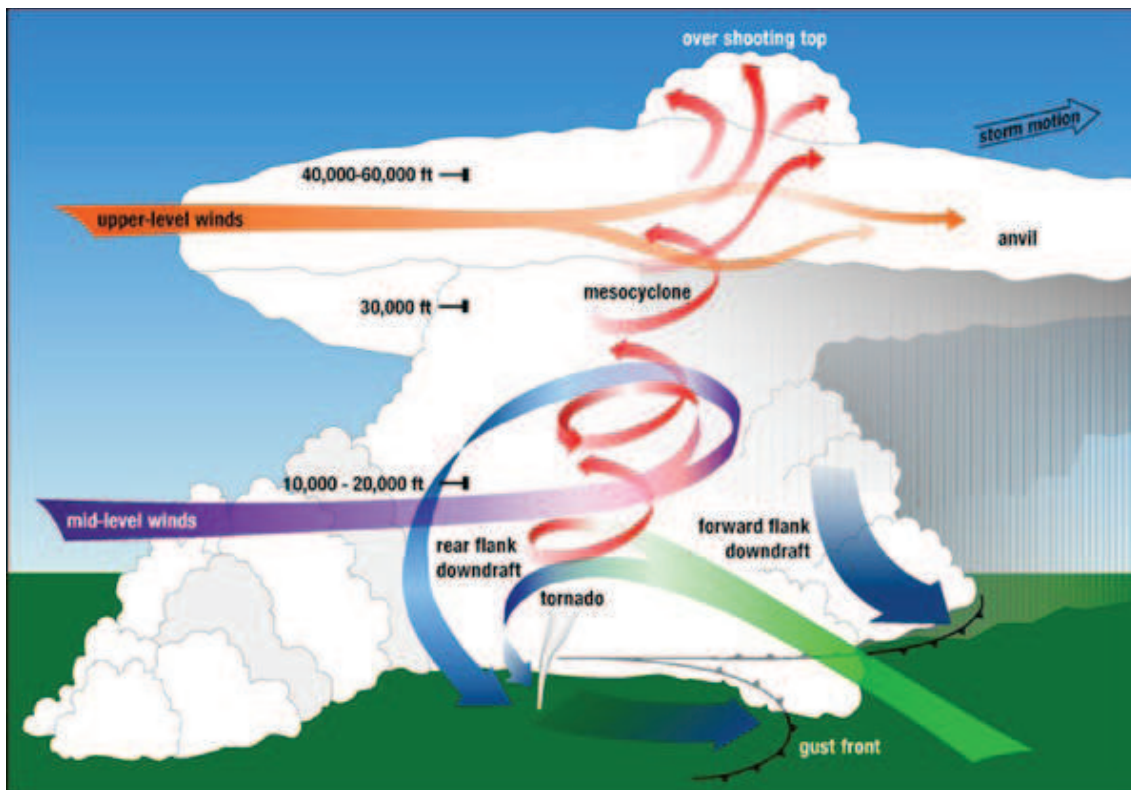
Figure 3: Structure of the supercell.

supercell thunderstorms are powerful sources of infrasound. Detailed observations show that almost all strong convective storms that have cloud tops greater that 14 km and which are capable of producing strong tornadoes generate significant infrasound in a passband from 0,5 to 2,5 Hz, with peak frequencies between 0,5 and 1 Hz (e.g. Bedard 2005; Bedard *et al.* 2004a). The acoustic power radiated could be as high as 10^7 watts (Georges 1988). These waves are strongly correlated with formation of tornadoes by supercell storms (Georges 1988), but they are not related with tornado itself and are caused by convective processes that precede tornado formation.

A supercell is a severe thunderstorm with a deep, continuously rotating updraft (a mesocyclone). Supercells are the largest and most severe quasi-steady-state storms as they can last for many hours and generate extreme weather. They are most frequent in the Great Plains of the United States, north-eastern India and eastern Australia, which are the areas that lie to the east of a moun-

tain range and poleward of a warm ocean. Supercells usually produce tornadoes, the most violent of atmospheric storms. Tornado is a violently rotating column of air, about 100 m in diameter, with wind speeds of approximately 130 m/s. There exist only few types of clouds that typically spawn tornadoes and although only third of supercells produce tornadoes, they are responsible for almost all violent and large tornadoes, which cause serious damage to inhabitants.

Supercells develop from the tilting of the horizontal vortices associated with the vertical shear of the environmental winds. Strong updrafts lift the air turning about a horizontal axis and cause this air to turn about a vertical axis. This forms the rotating updraft. Cloud top of severe storm can break through the troposphere and reach into the lower levels of the stratosphere. Environmental winds at the top of updraft blow out the cooled air, precipitation is not falling through the updraft and downdrafts and updrafts are separated. This is the reason of the supercells being quasi-steady and severe. Figure 3 shows the structure of the supercell.

The main goal of scientists is to provide early warning of tornadoes. Satellite data and weather radar are used in order to determine the structure of storms and their potential to cause severe weather. The "hook echo" on the diagram of supercell seen on weather radar indicates the presence of a mesocyclone and also the great possibility of supercell being tornadic. Infrasound measurements are provided by Continuous Infrasonic Network (ISNeT) operations. ISNeT operation collocated with a Doppler radar provides a unique dataset for comparing infrasonic measurements with well-observed storm kinematics. A number of American universities (University of Mississippi, Southern Methodist University, the University of California at San Diego, the University of Alaska at Fairbanks, and the University of Hawaii at Manoa) have active research programs in infrasound.
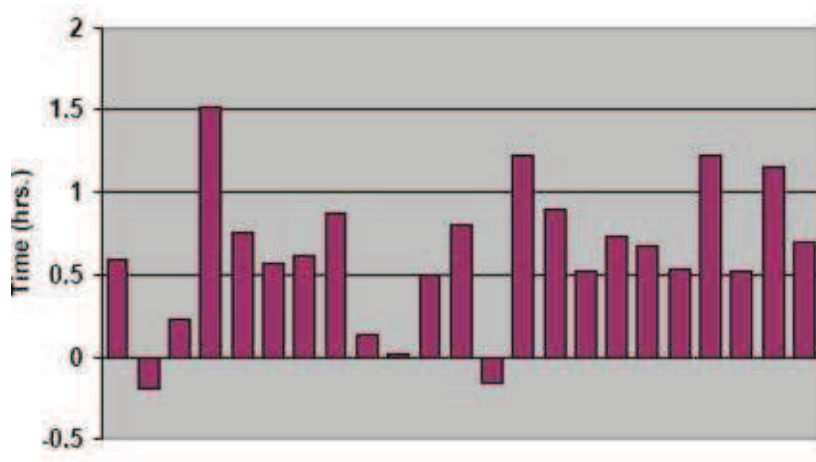
Figure 4: Histogram of the differences between predicted acoustic signal arrival times and the start times of infrasonic detection. This figure indicates that infrasound is usually produced well prior to reports if tornadoes.

Justification

Over the years several potential sound generation mechanisms were compared with the measured characteristics of the infrasound from strong convective storms (Georges and Greene 1975; Georges 1988; Bedard and Georges 2000; Beasley *et al.* 1976). Such mechanisms include release of latent heat, dipole radiation, boundary layer turbulence, lightning, electrostatic sources and vortex sound (radial vibrations and the co-rotation of suction vortices). Many sources were eliminated as likely candidates. One of the promising sources was quadrupole source of sound provided by interaction of turbulent vortices (Lighthill's quadrupole radiation), but acoustic power of this radiation leads to the underestimation (Georges and Greene 1975; Gossard and Hooke 1975; Schecter *et al.* 2008), since it requires that characteristic velocity of the turbulence is much greater than exists in any storm system.

Tornadic vortex core radial vibration was concluded to be the most likely model, but it can't explain sound emission 0.5 - 1 hrs before observation of tornado. Summarized differences between predicted acoustic signal arrival times from reported tornadoes and the start times of infrasonic detection show that infrasound is usually produced well prior (up to an hour) to reports of tor-

nadoes. Figure 4 is a histogram that shows the differences between predicted acoustic signal arrival times and the start times of infrasonic detection (Bedard *et al.* 2004b).

So, the physical mechanism of the process remains unexplained.

Infrasound of a tornadic thunderstorm is much stronger than infrasound of a nonsevere weather system and these waves are strongly correlated with formation of tornadoes. Therefore, potential sound generation mechanism is expected to explain observed high correlation between intensity of low frequency infrasound signals from supercell storms and the probability of later tornado formation. In other words this means that acoustic power of the infrasound source is required to depend on the same parameters that are the most promising in discriminating between nontornadic and tornadic supercells.

The study presented in the dissertation from our point of view contains significant results for the solution of above mentioned problems, namely, explanation of the physical mechanism responsible for infrasound emission from strong convective storms and observed high correlation between infrasound intensity and tornado formation.

The physical processes responsible for the Solar chromospheric heating is one of the major puzzles of solar physics. Neither of the mechanisms can account for amount of the energy needed for the heating of the whole chromosphere. Although these mechanisms can provide considerable contribution in chromospheric heating process, some other heating mechanisms are also necessary for complete explanation of the existing observations.

My study presented in this dissertation was partly motivated by chromospheric heating problem. Namely, it was suggested (and our preliminary estimates have partly confirmed this suggestion) that waves generated by turbulence in the partially ionized plasma of the solar chromosphere can play significant role in the chromospheric dynamics.

Aim of the research

The aim of the presented dissertation is extension of the Lighthill's acoustic analogy for the systems where stochastic heat and air mass fluctuations are presented (such as turbulence in saturated air or partially ionized plasma of the solar chromosphere with non-zero temperature fluctuations) and application of obtained results to infrasound generation in strong convective storms and explanation of observed high correlation between infrasound intensity and tornado formation. The aim of the ongoing research is application of developed theory to the study of wave generation processes is solar chromosphere and examination of its role in the heating of the solar atmosphere.

The broad and smooth spectra of the observed infrasound radiation from strong convective storms indicates that turbulence is one of the promising sources of the radiation. Application of the Lighthill's acoustic analogy (Lighthill 1952) for understanding the sound generation by turbulent flows gives the following results: In the case of uniform background thermodynamic parameters, interaction of turbulent vortices provides a quadrupole source of sound, while temperature fluctuations represent dipole sources of sound ("hot spots" or "entropy inhomogeneities" behave as scattering centers at which dynamic pressure fluctuations are converted directly into sound). In the case of stratified atmosphere there also exist dipole source related to stratification (Goldstein 1976) and monopole source related to variability of adiabatic index, that usually have negligible acoustic output (Howe 2001).

We study acoustic radiation from turbulent convection using Lighthill's acoustic analogy and taking into account the effects of stratification, temperature fluctuations and moisture in the air. From technical point of view the generalized acoustic analogy (Goldstein 2002) implies: (i) dividing the flow variables into their mean and fluctuating parts; (ii) subtracting out the equation for the mean flow; (iii) collecting all the linear terms on one side of equations and the

nonlinear terms on the other side; (iv) treating the latter terms as the known terms of sound.

Acoustic wave equation for turbulent flow describes not only acoustic waves, but also the instability wave solutions that are usually associated with large scale turbulent structures and continuous spectrum solutions related to "fine-grained" turbulent motions (Goldstein 2002; Goldstein 1984). In the presence of any kind of inhomogeneity, such as stratification or velocity shear, linear coupling between these perturbations is possible, and in principle acoustic waves can be generated by both instability waves and continuous spectrum perturbations. But in the case of low Mach number ($M \ll 1$) flows both kinds of perturbations are very inefficient sources of sound. The acoustic power is proportional to $e^{-1/2M^2}$ and $e^{-\pi\delta/2M}$ for instability waves and continuous spectrum perturbations respectively (Crighton and Huerre 1990). In the last expression δ is the ratio of length scales of energy containing vortices and background velocity inhomogeneity ($V/\partial_z V$). In the case of supercell thunderstorms $M \sim 0.1-0.15$ and $\delta \sim 10^{-2}$, therefore both linear mechanisms have negligible acoustic output and attention should be payed to sources of sound related to nonlinear terms and entropy fluctuations.

In the case of turbulent convection turbulent mixing of saturated air with different temperatures leads to nonstationary heat and mass production during the condensation of moisture.

Suppose there exist two saturated air parcels of unit mass with different temperatures T_1 and T_2 and water masses $m_\nu(T_1)$ and $m_\nu(T_2)$. Mixing of these parcels leads to the condensation of water due to the fact that

$$2m_\nu(T_1/2 + T_2/2) < m_\nu(T_1) + m_\nu(T_2). \tag{3}$$

Both of these effects, production of heat and decrease in the mass of the gas, are known to produce monopole radiation (Goldstein 1976; Howe 2001). Consequently, one can expect that these new sources could play important role in

sound generation by saturated moist air turbulence. We study various sources of acoustic radiation in a stratified, moist, turbulent atmosphere, analyze there characteristics, estimate total emissivities and apply obtained results to infrasound generation in strong convective storms for explanation of observed high correlation between infrasound intensity and tornado formation.

We also intend to apply the mechanism of acoustic wave generation by turbulence related to the non-stationary heat sources to the study of physical processes in the solar chromosphere (Akhalkatsi and Gogoberidze 2011). Solar atmosphere possess ionization zones with ionization degree as high as $(10^{-2}-10^{-4})$ in the upper chromosphere. The ionization degree depends on the temperature. Velocity fluctuations invoke mixing of partially ionized plasma from different regions of the chromosphere, which causes temperature fluctuations and, consequently, initiates fluctuations of the ionization level. Like saturated moist air in the Earth's atmosphere, non-stationary heat fluctuations related to the partial ionization of solar atmosphere produce monopole sources of acoustic and gravitational waves. We will analyze the role of this mechanism in the both chromospheric and coronal heating in the Sun and other cool stars of solar type that have a partially ionized chromosphere.

Main results

The main results of dissertation are as follows:

1. Acoustic wave generation by turbulence in a stratified, moist atmosphere is studied in the framework of a generalized acoustic analogy. It is shown that in saturated moist air turbulence in addition to the Lighthill's quadrupole and dipole sources of sound (related to stratification and temperature fluctuations), there exist monopole sources related to heat and mass production during the condensation of moisture.

2. The acoustic power of these monopole sources is determined and it is

shown that this radiation is dominant for typical parameters of strong convective storms. The results are in good qualitative agreement with the main observed characteristics of infrasound radiation by strong convective storms, such as total acoustic power and characteristic frequency.

3. It is estimated that the total power of the source related to moisture is of order 10^7 watts, in qualitative agreement with observations of strong convective storms.

4. It is shown that for typical parameters of strong convective storms the peak frequency of infrasound radiation is $\nu_{peak} \approx 0.8$ Hz, which is in a good agreement with observations.

5. Detailed spectral analysis of a monopole source of sound related to the heat production during the condensation of moisture are performed.

6. A quantitative explanation of the correlation between intensity of infrasound generated by supercell storms and later tornado formation is given. It is shown that low lifting condensation level (LCL) and high values of convective available potential energy (CAPE), which are known to favor significant tornadoes, also lead to a strong enhancement of supercells low frequency acoustic radiation.

Novelty and practical utility

The dissertation includes new results in aeroacoustics and physics of mesoscale convective systems. Concerning to aeroacoustics novelties include finding of new monopole sources of sound related to heat and mass production during the condensation of moisture in saturated moist turbulent medium. Besides, it is shown that the acoustic power of a monopole source of sound related to the heat production during the condensation of moisture is dominant for typical parameters of strong convective storms. Dissertation also includes a quantitative explanation of the correlation between intensity of infrasound generated by

supercell storms and later tornado formation. Acoustic power of a monopole source related to the moisture of the air strongly depends on the same parameters that are the most promising in discriminating between nontornadic and tornadic supercells according to the recent study of tornadogenesis. The strong correlation between the intensity of infrasound signals from supercell storms and probability of later tornado formation indicates the potential for improving tornado forecasting and reducing false alarms from non-tornadic supercells by combining ISNeT (Infrasonic Network) data with the information from Doppler Radar. It should be noted that developed theory opens wide perspectives for future theoretical, numerical, as well as observational research in mesoscale convective system dynamics and promotes better understanding of physical processes in strong convective systems.

We also believe that this novel mechanism of wave generation by turbulence related to the non-stationary heat sources, when applied to the partially ionized plasma of the solar atmosphere, will give new results in solar physics and help in understanding of physical processes in the solar chromosphere.

Structure

Dissertation consists in Introduction, 4 section and Conclusion.

In **section 1** wave generation by turbulent convection is considered and acoustic analogy is introduced. Extended theory of acoustic analogy is analyzed to include the effects of stratification and the solar p-Modes are considered.

In **subsection 1.1** Lighthill's acoustic analogy is introduced. Formulation of the acoustic analogy implies: (i) dividing the flow variables into their mean and fluctuating parts; (ii) subtracting out the equation for the mean flow; (iii) collecting all the linear terms on one side of equations and the nonlinear terms on the other side; (iv) treating the latter terms as the known terms of sound.

Lighthill's quadrupole source is discussed in **subsection 1.2**. Mathematical

methods used for farther analysis are considered.

Stein's (1967) theory of acoustic and gravity wave generation by turbulence in a stratified atmosphere is considered in **subsection 1.3**. It is emphasized that wave emission by turbulent convection is a common process in stellar convective zones and it is clearly implicated in the heating of stellar chromospheres and coronas.

The inhomogeneous wave equation is discussed in **sub-subsection 1.3.1** and solution of this equation is given in **sub-subsection 1.3.2**. It is shown that stratification cuts off the acoustic radiation at low Mach numbers and that the gravity wave emission peaks near some critical angle to the vertical.

Estimates of the total acoustic power and the gravity-wave energy flux are given in **sub-subsection 1.3.3**.

Wave generation by turbulent convection is considered in **subsection 1.4**.

In **sub-subsection 1.4.1** the model atmosphere proposed by Goldreich and Kumar (1990) and wave types are introduced. This model of a plane parallel, stratified atmosphere consists of two semi-infinite layers, the lower adiabatic and the upper isothermal. The normal wave modes are classified as trapped or propagating, and as composed of acoustic or gravity waves.

Wave mode excitation by turbulent convection and monopole, dipole and quadrupole source terms in the adiabatic layer are discussed in **sub-subsection 1.4.2**. These sources appear from the expansion and contraction of fluid due to the gain and loss of specific entropy, buoyancy force variations associated with these entropy changes, and momentum transport by the fluctuating Reynold's stress.

Characteristics and the excitation rate for trapped acoustic modes, or p-Modes, are given in **sub-subsection 1.4.3**.

Solar p-Modes are discussed in **sub-subsection 1.4.4**. It is shown that the theoretical results obtained for the amplitudes and linewidths of the solar p-Modes match the observational ones in the upper part of the solar convection

zone. This agreement supports the hypothesis that the solar p-Modes are stochastically excited by turbulent convection.

Generation of trapped and propagating waves is discussed in **sub-subsection 1.4.5**.

Discussion and summary is given in **subsection 1.5**.

Acoustic wave generation by turbulence in stratified, moist atmosphere is studied in **section 2**.

Equations governing the sound generation by turbulence for moist atmosphere are obtained in **subsection 2.1** in the framework of Lighthill's acoustic analogy and taking into account effects of stratification, temperature fluctuations and moisture in the air.

Various sources of acoustic radiation are analyzed in **subsection 2.2**. It is shown that in addition to the Lighthill's quadrupole and known dipole sources of sound related to stratification and temperature fluctuations there exist monopole sources related to heat and mass production during the condensation of moisture in the saturated moist air turbulence.

Obtained results are applied to infrasound generation in strong convective storms in **subsection 2.3**. It is shown that for typical parameters of the strong convective storms infrasound radiation should be dominated by monopole sources related to the moisture of the air. The results are in good qualitative agreement with the main observed characteristics of infrasound radiation by strong convective storms, such as total acoustic power and characteristic frequency.

Conclusions of the section are given in **subsection 2.4**.

Section 3 represents an extension of the study performed in **section 2** in two directions. Firstly, the generation of acoustic waves by turbulent convection is considered and spectral analysis of a monopole source of sound related to the heat production by condensation of moisture is performed. Secondly, a quantitative explanation of the correlation between intensity of infrasound

generated by supercell storms and later tornado formation is given.

General formalism is presented in **subsection 3.1**.

Detailed spectral analysis of a monopole source of sound related to heat production during condensation of moisture, which is supposed to be dominant in the infrasound radiation observed from strong convective storms, is performed in **subsection 3.2**. Assuming homogeneous and stationary turbulence the spectrum of acoustic radiation is calculated.

Detailed analysis of the sound generated by a monopole source as well as infrasound observations are performed in **subsection 3.3**. Correlation between intensity of infrasound radiation by supercell storm and probability of tornado formation is discussed. It is shown that low lifting condensation level (LCL) and high values of convective available potential energy (CAPE), which are known to favor significant tornadoes, also lead to a strong enhancement of supercells low frequency acoustic radiation. Particularly, low LCL implies warmer air at the level of saturation. Increase of temperature causes rapid enhancement of acoustic power. High values of CAPE mean high updraft velocity and therefore, increased rms of turbulent velocities. This results in strong enhancement of total acoustic power.

Conclusions of the section are given in **subsection 3.4**.

Main solar chromospheric heating mechanisms are reviewed in **section 4**. The physical processes responsible for the solar chromospheric heating is a major puzzle of solar physics since it is found that the temperature in the solar chromosphere is much higher than that can be expected for a plasma in radiative equilibrium. It is emphasized that neither of the mechanisms reviewed can account for amount of the heat needed for the heating of the whole chromosphere.

Two complementary approaches, semiempirical and theoretical, that are used for understanding the solar and stellar atmospheres, are introduced in **subsection 4.1**. Empirically derived parameters of solar atmosphere from one-

dimensional model of the solar atmosphere (called SRPM 306) of the quiet-Sun chromosphere are shown.

The ongoing study of applying the novel mechanism of acoustic wave generation by turbulence related to the non-stationary heat sources presented in **section 2** to Solar chromospheric heating is discussed in **subsection 4.2**. It is suggested that the role of acoustic and gravity waves generated by heat fluctuations related to the partial ionization of chromosphere can have significant contribution to both chromospheric and coronal heating of the Sun and solar type stars.

Conclusions of the section are given in **subsection 4.3**.

1 Generation of waves by turbulence and the origin of solar p-Modes

In this section wave generation by turbulence is considered and acoustic analogy is introduced. Extended theory of acoustic analogy is analyzed to include the effects of stratification. Different features and generation mechanisms of solar p-Modes are considered.

1.1 Lighthill's acoustic analogy

Lighthill (1952) introduced acoustic analogy approach to calculate acoustic radiation from relatively small regions of turbulent flow embedded in an infinite homogeneous fluid in which the speed of sound and the density are constant. The dynamics of the flow is governed by the continuity and momentum equations:

$$\frac{D\rho}{Dt} + \rho \nabla \cdot \mathbf{v} = \rho q, \tag{4}$$

$$\rho \frac{D\mathbf{v}}{Dt} = -\nabla p + \nabla \sigma + f, \tag{5}$$

where $\mathbf{v}$, ρ and p are velocity, density and pressure respectively; σ is a viscous stress tensor. $D/Dt \equiv \partial/\partial t + \mathbf{v} \cdot \nabla$ is Lagrangian time derivative; An external volume flow source q within the fluid and an externally applied volume force f are added to continuity and Navier-Stokes equations respectively in order to clearly show the nature of different sources. It is assumed that these source terms cause no entropy production.

Using the continuity equation (4) we can obtain the momentum equation in conservation form:

$$\frac{\partial \rho v_i}{\partial t} + \frac{\partial (\rho v_i v_j)}{\partial x_j} = -\frac{\partial p}{\partial x_j} + \frac{\partial \sigma}{\partial x_j} + \rho q v_i + f_i. \tag{6}$$

Taking the time derivative of the mass equation (4) and subtracting from this the divergence of the momentum equation (6) we obtain:

$$\frac{\partial^2 \rho}{\partial t^2} = \frac{\partial^2 (\rho v_i v_j - \sigma_{ij})}{\partial x_i \partial x_j} + \frac{\partial^2 p}{\partial x_i^2} + \frac{\partial (\rho q)}{\partial t} - \frac{\partial (\rho q v_i + f)}{\partial x_i}. \tag{7}$$

Subtracting on both sides of this equation a term $c_s^2 (\partial^2 \rho / \partial x_i^2)$ provides this equation the form of the inhomogeneous wave equation:

$$\frac{\partial^2 \rho}{\partial t^2} - c_s^2 \frac{\partial^2 \rho}{\partial x_i^2} = \frac{\partial^2 (\rho v_i v_j - \sigma_{ij})}{\partial x_i \partial x_j} + \frac{\partial^2 (p - c_s^2 \rho)}{\partial x_i^2} + \frac{\partial (\rho q)}{\partial t} - \frac{\partial (\rho q v_i + f)}{\partial x_i}, \tag{8}$$

where c_s is the speed of sound:

$$c_s \equiv \left(\frac{\partial p}{\partial \rho} \right)_s^{1/2}. \tag{9}$$

In general equation (8) is useless, as it is an equation with twelve unknowns (for a simple fluid σ_{ij} is symmetrical).

The key idea is to compare this equation with the equation for the perturbation of a uniform and stagnant fluid in the state (ρ_0, p_0). We consider an unsteady disturbance with characteristic length λ traveling at a propagation speed whose typical value is c_s through a fluid in which the velocity, pressure, and density are otherwise determined by the equations of a steady flow. Such a disturbance will introduce changes in velocity, pressure, density, entropy, and c_s^2 ($\mathbf{v}' = \mathbf{v} - \mathbf{v_0}, p' = p - p_0, \rho' = \rho - \rho_0, s' = s - s_0$) as it passes by a fixed observer. These changes will all occur on the time scale $T_p = 1/f$, where $f = c_s/\lambda$ is the characteristic frequency of the disturbance. We identify c_s as the speed of sound in the stagnant uniform fluid surrounding the listener. We can further define the perturbations ρ' and p' as the differences between the local values of ρ and p and the values of these quantities in the reference fluid surrounding the listener (5). In this generalization the amplitude of the disturbance measured be the magnitude of perturbations do not need to be small. As ρ_0 and p_0 are like c_s constant we can write Lighthill's equation (8) as:
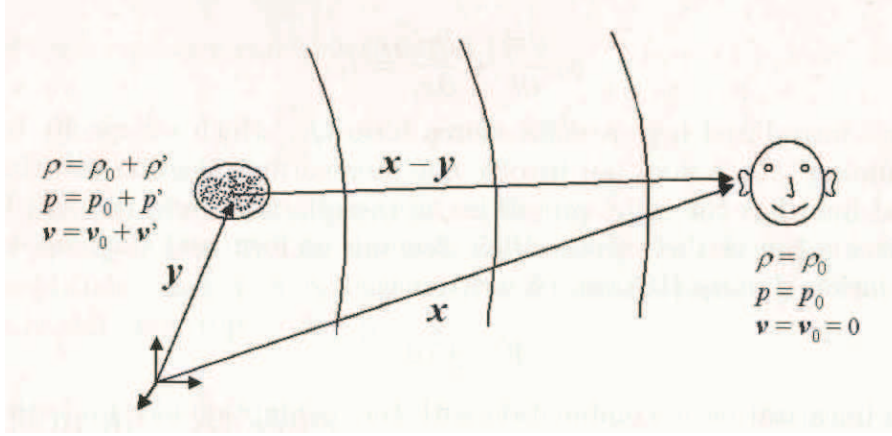
Figure 5: Source and listener in the analogy of Lighthill. While in the source region the density fluctuations are not necessarily small, around the listener an acoustical behavior with $\rho' \ll \rho_0$ is assumed.

$$\frac{\partial^2 \rho'}{\partial t^2} - c_s{}^2 \frac{\partial^2 \rho'}{\partial x_i^2} = \frac{\partial(\rho q)}{\partial t} - \frac{\partial(\rho q v_i + f)}{\partial x_i} + \frac{\partial^2 T_{ij}}{\partial x_i \partial x_j}, \qquad (10)$$

where it is assumed that external volume flow source q does not involve any momentum injection and that the injected fluid has the same properties as the reference fluid (ρ_0, p_0). Hereafter the specific case with $\mathbf{v_0} = 0$ is considered.

In Eq. (10)

$$T_{ij} = \rho v_i v_j + \delta_{ij}(p' - c_s^2 \rho') - \sigma_{ij} \qquad (11)$$

is *Lighthill's turbulence stress tensor* and $\rho v_i v_j$ is the Reynolds stress. The second term is the excess of momentum transfer by the pressure over that in an ideal fluid of density ρ_0 and sound speed c_s. This is caused by wave amplitude nonlinearity and by mean density variations in the source flow. The viscous stress tensor σ_{ij} is linear in the perturbation quantities and properly accounts for the attenuation of the sound.

Higher order terms, having higher order derivatives aren't included in this equation, because they have negligible contribution, when far field approximation is used.

The left hand side of Eq. (10) is the wave operator of the homogeneous

acoustic wave equation, which, in the absence of externally applied forces or moving boundaries, has only the trivial solution $\rho' = \rho - \rho_0 = 0$, because the radiation condition ensures that sound waves cannot enter from infinity. Lighthill's analogy implies an identification of the right hand side of this equation as a known source of sound. The sound generated in the real fluid may now be considered equivalent to that produced in an ideal, stationary acoustic medium that is forced by the source terms on the right hand side of Eq. (10). The problem of calculating the aerodynamic sound is therefore formally equivalent to solving this equation for the radiation into a stationary, ideal fluid produced by a distribution of source terms that vanish at large distances from the flow, i.e., the source region is very small relative to the wavelength of emanated sound. A source distribution satisfying this condition is said to be compact.

The first term on the right hand side of the wave equation is a monopole source of sound, which is produced by compact flow source and acts as if its entire strength were concentrated at a single point. The second term is a dipole source produced by an external volume force. This term can be treated as being composed of two equal-strength monopoles with opposite signs that have been brought together.

The third term, Lighthill's source, produces the acoustic field exactly equivalent to the emission of the quadrupole source, whose strength per unit volume is the Lighthill turbulence stress tensor T_{ij}. Quadrupole source can be thought as composed of two dipoles that are of equal strength but have opposite sign. Therefore, there is an exact analogy between the density fluctuations that occur in any real flow and the small amplitude density fluctuations that would result from a quadrupole source distribution (of strength T_{ij}) in a fictitious acoustic medium with sound speed c_s.

Lighthill's equation (10) is an exact consequence of the laws of conservation of mass and momentum and it must be satisfied by all real flows. Even

for those flows that are sound-like T_{ij} accounts not only for the generation of sound, but also for all effects which occur whenever acoustic waves interact with moving flows (self-modulation due to acoustic nonlinearity, convection by the flows, refraction due to sound speed variations, and attenuation due to thermal and viscous actions) and which, therefore, can not be predicted without some knowledge of the sound field. Nonlinear effects on propagation and dissipation are usually sufficiently weak to be neglected within the source region, although they may affect propagation to a distant observer. Convection and refraction of sound within and near the source flow can be important, for example when the sources are contained in a turbulent shear layer, or are adjacent to a large, quiescent region of fluid whose mean thermodynamic properties differ from those in the radiation zone. Effects of this kind are accounted for by contribution to T_{ij} that are linear in the perturbation quantities relative to a mean background flow. Thus, a knowledge of T_{ij} is, in effect, equivalent to solving the complete nonlinear equations governing the flow motion, which is virtually impossible for most flows of interest.

Nevertheless, we are usually content with approximate indications of the acoustic filed magnitude and suggestions about its dependance on parameters and have no need for its highly accurate predictions. Moreover, there are certain types of flows where it is often possible to obtain fairly good estimates of T_{ij} and, consequently, good estimates of the sound field. In addition, acoustic analogy approach allows us to utilize the powerful tools of classical acoustics. Lighthill's analysis regards the source terms as a quantities about which we have at least some prior knowledge. Since aerodynamic sound sources of practical interest are very often acoustically compact, the far field solutions of the Lighthill's equation will automatically account for the extreme inefficiency of these sources and will provide reasonable estimates of the acoustic field even when they are not precisely known.

Practical utility of Lighthill's equation rests on the regarding the right side

of the equation as known source terms that vanish at large distances from the flow and on the hypothesis that all the effects, which occur whenever acoustic waves interact with moving flows, can be ignored. Below the reasonableness of these assumptions is shown.

Within the subsonic turbulent flow of relatively small spatial extent embedded in a uniform stationary atmosphere viscous stress σ_{ij} makes a much smaller contribution to T_{ij} than the Reynolds stress term $\rho v_i v_j$, because the ratio of these terms is of the order of magnitude of the Reynolds number ul/ν, which in virtually all applications of aerodynamic noise theory is quite large.

At sufficiently large distances from the flow acoustic approximation implies that velocity v_i is small and Reynolds stress term $\rho v_i v_j$ is negligible. Moreover, the effects of viscosity and heat conduction only cause a slow damping due to the conversion of acoustic energy into heat and have a significant effect only over very large distances. Thus, σ_{ij} can be entirely neglected for distances of propagation comparable to the wavelength.

Functional relationship between the pressure p, density ρ and the specific entropy s (entropy per unit mass) is given by assuming that the fluid maintains itself in a state of local thermodynamic equilibrium (i.e., that relaxation effects can be neglected). Then, since any thermodynamic property can be expressed as a function of any two others, i.e., by an equation of state:

$$p = p(\rho, s). \tag{12}$$

In the differential form it yields:

$$\frac{Dp}{Dt} = c_s^2 \frac{D\rho}{Dt} + \left(\frac{\partial p}{\partial s}\right)_\rho \frac{Ds}{Dt}. \tag{13}$$

Whenever the flow emanates from a region of uniform temperature and the heat transfer, which is of the same order of magnitude as the viscous effects, is relatively unimportant, the reference fluid remains uniform and stagnant so
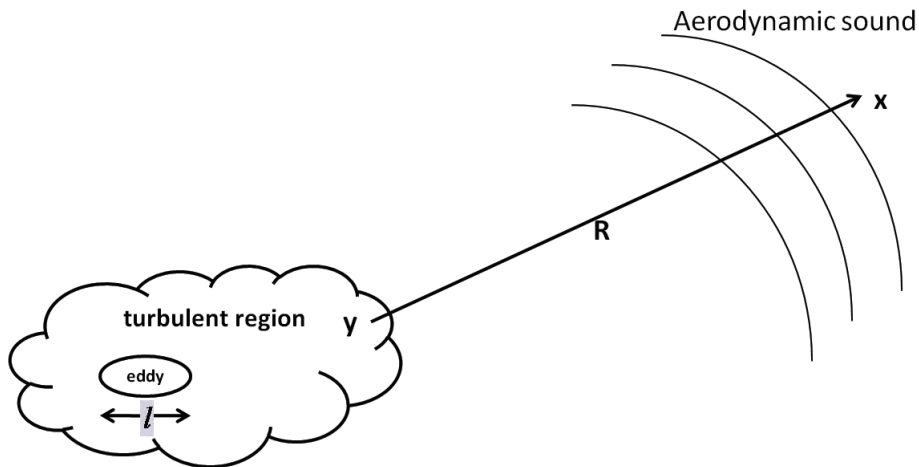
Figure 6: Aerodynamic sound in an unbounded fluid.

that the entropy is relatively constant and the equation of state (13) can be written as

$$p' = c_s^2 \rho'. \tag{14}$$

These assumptions show that the Reynolds stress T_{ij} is approximately equal to $\rho v_i v_j$ inside the flow and approximately equal to zero outside this region. When the mean density and sound speed are uniform, the density fluctuations in ρ produced by low Mach number, high Reynolds number fluctuations are of order $\rho_0 M^2$, and, hence, they are negligible. Thus,

$$T_{ij} \simeq \rho_0 v_i v_j. \tag{15}$$

Since only a very small fraction of the energy in the flow gets radiated as sound, it is reasonable to suppose that the source terms can be determined from measurements or estimates of the turbulence, without any prior knowledge of the sound field. Then the right side of Lighthill's Eq. (10) can be treated as known source terms.

1.2 Lighthill's quadrupole source

In the previous section Lighthill's acoustic analogy was introduced and it was shown that the problem of predicting the sound emission from a region of unsteady flow embedded in a uniform atmosphere can be reduced to the classical problem of predicting the sound field from known sources of limited spatial extent. In the absence of external volume flow source q (monopole terms) and an external volume force f (dipole terms) the leading order term in the sound field produced by a free turbulent flow is the Lighthill's quadrupole term. In this section solution of Lighthill's Eq. (10) for Lighthill's source is introduced.

Using Eqs. (10) and (14) we can rewrite the Lighthill's equation for quadrupole source to obtain

$$\frac{1}{c_s{}^2}\frac{\partial^2 p'}{\partial t^2} - \frac{\partial^2 p'}{\partial x_i^2} = \frac{\partial^2 T_{ij}}{\partial x_i \partial x_j}, \tag{16}$$

where we use the pressure fluctuations p' as aero-acoustic variable.

The pulse emitted from an acoustic source located at the point $\mathbf{y}$ travels the distance $\mathbf{R}$ in the time $\mathbf{R}/c_s$ (see Fig. 6). Thus, the time at which the signal arriving at the point $\mathbf{x}$ at the time t was emitted from the point $\mathbf{y}$ is represented by $t - (\mathbf{R}/c_s)$. It is called the *retarded time.*

The most convenient way to obtain a better approximation for the effect of retarded time differences across the source region is to use the free space Green function

$$G_0(t, \mathbf{x}|\tau, \mathbf{y}) = \frac{\delta(t - \tau - |\mathbf{x} - \mathbf{y}|/c_s)}{4\pi c_s{}^2|\mathbf{x} - \mathbf{y}|}, \tag{17}$$

which is solution of the equation:

$$\left(\nabla^2 - \frac{1}{c_s{}^2}\frac{\partial^2}{\partial t^2}\right)G_0 = -\delta(t - \tau)\delta(\mathbf{x} - \mathbf{y}) \tag{18}$$

and has the symmetry property

$$\frac{\partial G_0}{\partial x_i} = -\frac{\partial G_0}{\partial y_i} \tag{19}$$

for differentiation with respect to the source coordinate $\mathbf{y}$ and the observer coordinate $\mathbf{x}$ (see Fig. 6).

The solution of Lighthill's equation (16) expressed in terms of the free space Green's function is given by

$$p'(\mathbf{x}, t) \approx c_s^2 \int_{-\infty}^{t} \int G_0(t, \mathbf{x}|\tau, \mathbf{y}) \frac{\partial^2 (\rho_0 v_i v_j)}{\partial y_i \partial y_j} d^3\mathbf{y} d\tau. \tag{20}$$

By partial integration we can move the space derivative from the source term $\partial^2(\rho v_i v_j)/\partial y_i \partial y_j$ (which we do not know accurately) toward the well known Green's function. Using the symmetry property (19) we can replace the derivatives of G_0 with respect to the source coordinate $\mathbf{y}$ by derivatives with respect to the observer coordinate $\mathbf{x}$. As the integration is performed on the source coordinate, we can move this spatial derivatives out of the integral, and obtain the integral formulation

$$p'(\mathbf{x}, t) \approx \frac{\partial^2}{\partial x_i \partial x_j} \int \frac{\rho_0 v_i v_j(\mathbf{y}, t - |\mathbf{x} - \mathbf{y}|/c_s)}{4\pi |\mathbf{x} - \mathbf{y}|} d^3\mathbf{y}, \tag{21}$$

where the integration with respect to τ is carried out and $t - |\mathbf{x} - \mathbf{y}|/c_s$ is the retarded time.

Assuming a compact source and the far field ($|\mathbf{x}| \gg |\mathbf{y}|$) approximation we can use the following expansions:

$$|\mathbf{x} - \mathbf{y}| \approx |\mathbf{x}| - \frac{\mathbf{x} \cdot \mathbf{y}}{|\mathbf{x}|}, \tag{22}$$

$$\rho_0 v_i v_j(\mathbf{y}, t - |\mathbf{x} - \mathbf{y}|/c_s) \approx \rho_0 v_i v_j \left(t - \frac{|\mathbf{x}|}{c_s} \right) + \frac{\mathbf{x} \cdot \mathbf{y}}{c_s |\mathbf{x}|} \frac{\partial}{\partial t} \rho_0 v_i v_j \left(t - \frac{|\mathbf{x}|}{c_s} \right), \tag{23}$$

and using plane wave approximation for far field derivatives

$$\frac{\partial}{\partial x_i} \approx -\frac{x_i}{c_s |\mathbf{x}|} \frac{\partial}{\partial t}, \tag{24}$$

for the Lighthill source we obtain

$$p'(x,t) = -\frac{\rho_0 x_i x_j}{4\pi c_s^2 |\mathbf{x}|^3} \frac{\partial^2}{\partial t^2} \int v_i v_j d^3 \mathbf{y}. \tag{25}$$

The order of magnitude of p' can be estimated in terms of the characteristic velocity v and length scale l of energy containing turbulent eddies in the source region (see Fig. 6). Fluctuations in $v_i v_j$ in different regions of the turbulent flow separated by distances greater then l tend to be statistically independent, and therefore generation of sound can be considered as a collection of F/l^3 independent eddies, where F is the volume occupied by the turbulence. The dominant frequency of the motion is $\sim v/l$, so the wavelength of the radiated sound is $\lambda \sim l/M_t$, where $M_t \equiv v/c_s \ll 1$ is turbulent Mach number. Therefore, each eddy is acoustically compact. Acoustic pressure generated by single eddy is $p_1' \sim (l/|\mathbf{x}|)\rho_0 v^2 M_t^2$, and the acoustic power it radiates is $N_1 \sim 4\pi|\mathbf{x}|^2 p_1'^2/\rho_0 c_s \approx \rho_0 v^3 l^2 M_t^5$, which corresponds to Lighthill's eighth power law. For total acoustic power this yields Proudman's estimate (Proudman 1952),

$$N \sim \frac{\rho_0 v^8}{l c_s^5} F. \tag{26}$$

This equation shows that acoustic output of the turbulent system strongly depends on the rms turbulent velocity (proportional to its eights power) and inversely proportional to the characteristic lengthscale of the energy containing eddies.

1.3 Wave generation by turbulence in a stratified atmosphere. Solar g-Modes

Lighthill's method of calculating the aerodynamic emission of sound waves is developed for the homogeneous medium. However, in the atmosphere of the Sun the characteristic size of turbulent eddies is considered to be comparable to the scale height of the stratification produced by gravity. Stein (1967) extended

Lighthill's theory to calculate acoustic and gravity-wave emission by turbulent motions in a stratified medium. He showed that stratification cuts off the acoustic emission at low Mach numbers and acoustic waves cannot propagate below the critical frequency $\omega_{ac} = c_s/2H$ (Lamb 1945). The gravity emission is anisotropic and peaks near the critical angle to the vertical $\theta_c = \cos^{-1}\omega/\omega_b$, where $\omega_b^2 = (\gamma - 1)/\gamma^2(c_s/H)$ and gravity waves cannot propagate above ω_b. Here H is the scale hight at the atmosphere and γ is the ratio of specific heats c_p/c_v. In addition, stratification acts as a boundary surface in the homogeneous case (Curle 1955) giving rise to dipole and monopole terms in the source function. Stein (1967) calculated the acoustic power output and the upward gravity flux. He concluded that on the Sun, gravity-wave emission is much more efficient than acoustic, but can occur only from turbulent motions in convectively stable regions, whereas acoustic waves are produced by turbulence in the entire convective zone.

1.3.1   The inhomogeneous wave equation

In a gravitationally stratified atmosphere, buoyancy as well as pressure acts as a restoring force for fluid oscillations, and two types of waves - acoustic and gravity waves - occur, depending on the dominant restoring force. Wave equation for the pressure fluctuations in an unbounded isothermal stratified atmosphere (Stein 1967) in terms of variable

$$P' = P_1/P_0^{1/2} \tag{27}$$

is:

$$\left[\frac{\partial^2}{\partial t^2} - c_s^2 \nabla^2 + \omega_{ac}^2 - \left(\frac{\partial}{\partial t} \right)^{-2} c_s^2 \omega_b^2 \nabla_1^2 \right] P' = \gamma^{1/2} c_s S, \tag{28}$$

where the source function is

$$\gamma^{1/2} c_s S = P_0^{1/2} \left[c_s^2 \left(1 + \left(\frac{\partial}{\partial t} \right)^{-2} \omega_b^2 \right) \left(-\nabla \cdot \mathbf{f} + \frac{\partial q}{\partial t} \right) \right.$$
$$\left. + \left(1 + \left(\frac{\partial}{\partial t} \right)^{-2} \mathbf{g} \cdot \nabla \right) \left\{ (\gamma - 1) \mathbf{g} \cdot \mathbf{f} - \frac{\partial}{\partial t} \left(c_s^2 q - h \right) \right\} \right]. \qquad (29)$$

Here $\mathbf{g} = (0, 0, -g)$ is the gravitational acceleration,

$$\omega_{ac} = c_s/2H \qquad (30)$$

is the critical frequency (Lamb 1945),

$$\omega_b = \left(\sqrt{\gamma - 1}/\gamma \right) c_s/H \qquad (31)$$

is the Brunt-Väisälä frequency and ∇_1 is the gradient in the horizontal direction.

q, $\mathbf{f}$ and h represent the collection of the non-linear terms

$$q = -\nabla \cdot (\rho_1 \mathbf{u}), \qquad (32)$$

$$\mathbf{f} = -\frac{(\rho \mathbf{u} u_j)}{\partial x_j} - \frac{(\rho_1 \mathbf{u})}{\partial t}, \qquad (33)$$

$$h = -\mathbf{u} \cdot \nabla P_1 - \gamma P_1 \nabla \cdot \mathbf{u}. \qquad (34)$$

from momentum and mass conservation equations and from the equation of adiabatic motion:

$$\frac{\partial p}{\partial t} + \mathbf{u} \cdot \nabla(P_0 + P_1) = c_s^2 \frac{\partial \rho}{\partial t} + \mathbf{u} \cdot \nabla(\rho_0 + \rho_1). \qquad (35)$$

P_1 and ρ_1 represent perturbations of pressure and density about the undisturbed pressure P_0 and density ρ_0 of an unbounded isothermal atmosphere in hydrostatic equilibrium. Hence, the undisturbed pressure and density are stratified with hight as $\exp(-z/H)$, with scale height $H = P_0/\rho_0 g$.

The basic Eq. (28) for calculating the generation of acoustic and gravity waves by given fluid motions has two extra terms compared to the usual wave equation. The term ω_{ac}^2 arises from the effect of the stratification on the compressional restoring force, and the term $(\partial/\partial t)^{-2} c_s^2 \omega_b^2 \nabla_1^2$ arises from the gravitational restoring force.

1.3.2 Solution of the wave equation

The fluid fluctuations are composed of wave motions and a turbulent flow field, which is assumed her to be confined to a finite region of space. The source function S depends on the wave motions as well as on the given flow field. However, if the amplitude of the wave motions is much smaller than that of the turbulent motions, their contribution to the source function is negligible. In addition, for the Kolmogorov turbulence the Reynolds stresses dominate in the source function and non-adiabatic terms are negligible if the Mach number is less than 0.04. For other turbulence spectra the Reynolds stress terms dominate even at higher values of the Mach number.

For the wave motions in the far field, which are small compared to the turbulent motions and for the small Mach number the source function to lowest order (with respect to the small parameter M) is

$$
\gamma^{1/2} c_s S = P_0^{-1/2} \left[c_s^2 \left(1 + \left(\frac{\partial}{\partial t} \right)^{-2} \omega_b^2 \right) \nabla \cdot \nabla \cdot (\rho_0 \mathbf{u} \mathbf{u}) \right.
$$
$$
\left. + (\gamma - 1) g \left(1 + \left(\frac{\partial}{\partial t} \right)^{-2} \mathbf{g} \cdot \nabla \right) \nabla \cdot (\rho_0 w \mathbf{u}) \right], \tag{36}
$$

where $\mathbf{u}$ is the turbulent velocity and w is its vertical component.

For the solution of the inhomogeneous wave equation (28) we have (Kato 1966):

$$P'(\mathbf{x},t) = \frac{\gamma^2}{8\pi^2 c_s} \frac{\omega^2}{(\omega^2 - \omega_b^2)^{1/2}} \int \frac{S(\mathbf{x}',t)}{r(\omega^2 - \omega_b^2 \cos^2\theta)^{1/2}}$$

$$\times \exp\left\{i\omega(t-t') - i\frac{(\omega - \omega_{ac})^{1/2} (\omega^2 - \omega_b^2 \cos^2\theta)^{1/2}}{c_s} \frac{(\omega^2 - \omega_b^2 \cos^2\theta)^{1/2}}{(\omega^2 - \omega_b^2)^{1/2}} r\right\} d^3\mathbf{x}' dt', \quad (37)$$

where $r = |\mathbf{x} - \mathbf{x}'|$ and θ is the angle between $\mathbf{r}$ and the vertical direction. This expression, without considering any specific source function, implies, that waves propagate for $\omega > \omega_{ac}$ (acoustic waves), and in the interval $\omega_b > \omega > \omega_b \cos\theta$ (gravity waves), while waves are attenuated for $\omega_{ac} > \omega > \omega_b$ and $\omega < |\omega_b \cos\theta|$ (Moore and Spiegel 1964).

The mechanical energy flux in a stratified atmosphere, in lowest order (with respect to the small parameter M), is:

$$\mathbf{F} = P_1 \mathbf{u} = -\frac{c_s^2}{\gamma} \left[P' \left(\frac{\partial}{\partial t}\right)^{-1} \left\{ \nabla_1 P' + \frac{\left(\nabla_z - \frac{2-\gamma}{2} \frac{\mathbf{g}}{c_s^2}\right)}{\left(1 + \left(\frac{\partial}{\partial t}\right)^{-2} \omega_b^2\right)} P' \right\} \right], \quad (38)$$

where ∇_z in the vertical direction.

The Fourier transform of Eq. (38) gives the following expression for the energy flux in terms of the frequency and angle θ between the direction of propagation and the vertical direction

$$\mathbf{F}(\mathbf{x},\omega) = \lim_{T\to\infty} \frac{1}{T} \frac{8\pi^5}{|\mathbf{x}|^2 c_s} \left\{ \hat{\mathbf{x}} \frac{\tilde{\omega}}{\omega} \left[\frac{\omega^4}{(\omega^2 - \omega_b^2)(\omega^2 - \omega_b^2 \cos^2\theta)} \right]^{\frac{3}{2}} \right.$$

$$\left. -i\hat{\mathbf{z}} \frac{2-\gamma}{\gamma} \left(\frac{\omega\omega_{ac}}{\omega^2 - \omega_b^2}\right) \left[\frac{\omega^4}{(\omega^2 - \omega_b^2)(\omega^2 - \omega_b^2 \cos^2\theta)} \right] \right\} |S(\mathbf{k},\omega)|^2, \quad (39)$$

where $\tilde{\omega}^2 = \omega^2 - \omega_{ac}^2$, $\hat{\mathbf{x}}$ is the direction of propagation, $\hat{\mathbf{z}}$ is the vertical and $\cos\theta = \hat{\mathbf{z}} \cdot \hat{\mathbf{x}}$.

The first term in the brackets on the right hand side of Eq. (39) is real for acoustic waves ($\omega > \omega_{ac}$) and for gravity waves ($\omega_b > \omega > |\omega_b \cos\theta|$), and imaginary for non-propagating waves ($\omega_{ac} > \omega > \omega_b$ and $\omega < |\omega_b \cos\theta|$). The

second term is always imaginary and can be neglected. The flux vanishes as $\omega \to \omega_{ac}$ and has peak at $\omega \approx \omega_b$ and for gravity waves at the critical angle $\theta_c = \cos^{-1} \omega/\omega_b$. For ω slightly greater than ω_{ac} the flux is peaked in the vertical direction.

The source function (36) transformed into a multipole expansion is:

$$
S = \left[\left(1 - \frac{\omega_b^2}{\omega^2} + \frac{\omega_b^2}{\omega^2}\delta_{j3} \right) \frac{\partial^2(\rho_0^{1/2} u_i u_j)}{\partial x_i \partial x_j} \right.
$$
$$
\left. -2\frac{\omega_{ac}}{c_s} \left(\frac{1}{\gamma} - \frac{1}{2}\frac{\omega_b^2}{\omega^2} + \frac{1}{2}\frac{\omega_b^2}{\omega^2}\delta_{j3} \right) \frac{\partial(\rho_0^{1/2} u_j w)}{\partial x_j} + \frac{\omega_{ac}^2}{c_s^2}\left(\frac{2-\gamma}{\gamma}\right)\left(\rho_0^{1/2} w w\right) \right] .(40)
$$

The source-function term arising from internal fluid (Reynolds) stresses (the first term in quadratic brackets on the right hand side of Eq. (40)) is quadrupole (the second space derivative of a tensor), because these stresses produce equal and opposite forces on opposite sides of a given element of fluid; the volume of the fluid element remains constant, its center of mass moves uniformly, but its surface distorts. The external gravitational force produces a stratification and introduces additional dipole and monopole source terms (the second and third terms in Eq. (40)).

1.3.3 The total acoustic power and the gravity-wave energy flux

From dimensional analysis of Eqs. (28), (38) and (40) one can obtain the following expressions for the acoustic power emitted per unit volume arising from the (nth) multipole term (Lighthill 1952)

$$
P^{(n)} \propto \frac{\rho_0 v^3}{l} \left(\frac{v}{c_s}\right)^{2n+1} \omega'^{2n} \tag{41}
$$

at high frequencies

$$
k \approx \frac{\omega}{c_s} = \frac{\omega'}{c_s}\frac{v}{l}, \tag{42}
$$
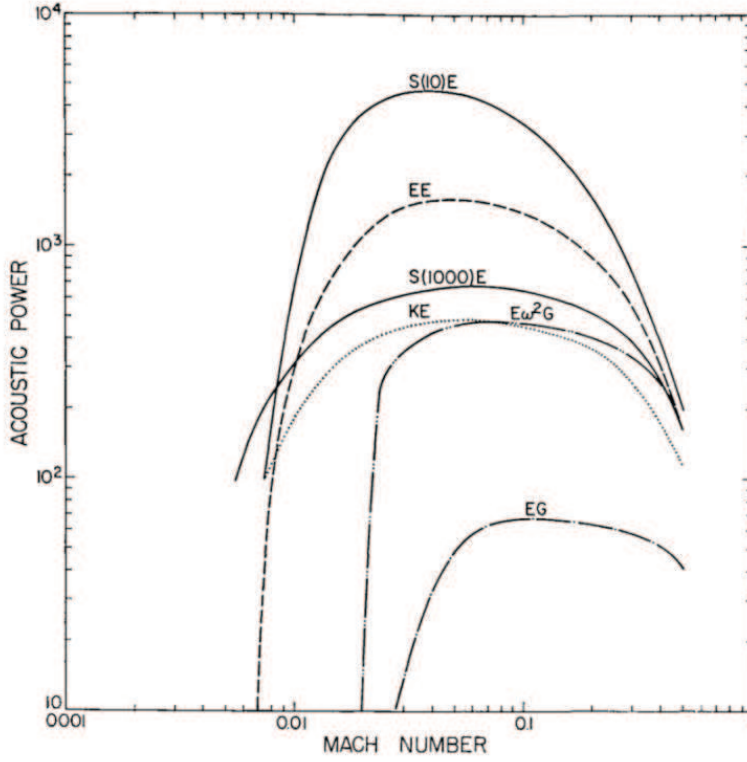
Figure 7: The non-dimensional total acoustic power output (in units of $(\rho_0 v^3/l)M^5$) as a function of turbulence Mach number, for several turbulence spectra.

where ω' is the dimensionless frequency and l/v is the time scale of the turbulence, and for the energy flux arising from the (nth) multipole term we have

$$F^{(n)} \propto \rho_0 v^3 \left(\frac{v}{c_s}\right) \left(\frac{l}{H}\right)^{2n} \left(\frac{l}{r}\right)^2 \qquad (43)$$

at low frequencies

$$k \approx \frac{\omega_{ac}}{c_s} = \frac{1}{H}. \qquad (44)$$

The total acoustic output per unit volume is approximately

$$P \approx 10^3 \frac{\rho_0 v^3}{l} M^5 ergs/cm^3 sec. \qquad (45)$$

The upward gravity wave flux emission per unit volume can be estimated as
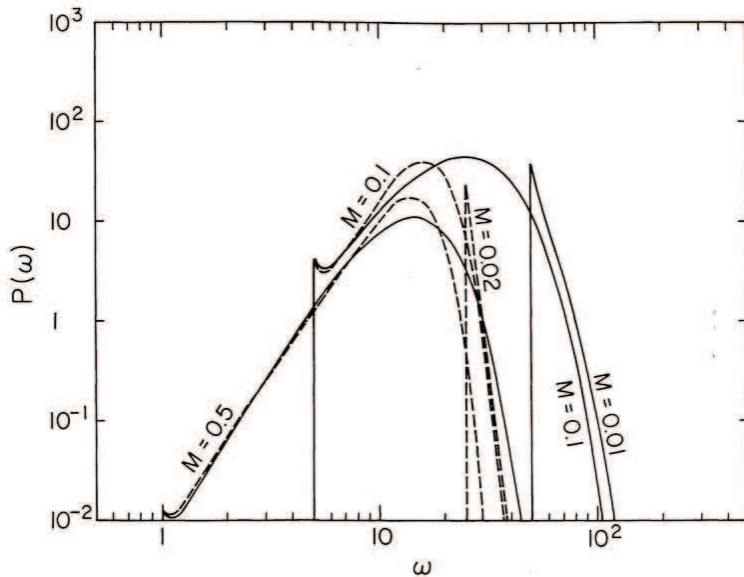
Figure 8: Non-dimensional acoustic power spectrum (in units of $\rho_0 v^2 M^5$) as a function of the dimensionless frequency (ω in units of v/l).

$$F_z \approx 10^2 \frac{\rho_0 v^3}{l}\left(\frac{l}{H}\right)^5 ergs/cm^2 sec. \tag{46}$$

The total acoustic output per unit volume, in units of $(\rho_0 v^3/l)M^5$, is shown as a function of Mach number in Figure 7, and its spectrum is shown in Figure 8. The vertical gravity-wave flux, in units of $(\rho_0 v^3/l)(l/H)^5$ for $l = H$, is shown in Figure 9 (Stein 1967).

The dimensionless acoustic power is roughly proportional to M^5 at intermediate Mach numbers and for $M = 0.1$ it is of the order of 100. It decreases as the Mach number approaches one and increases at small Mach numbers where the emission is very sensitive to the form of the turbulence spectrum (Fig. 7).

The sensitivity of the energy emission to the Mach number of the turbulence and the frequency of the waves [see Eq. (41)] arises because the opposite motions from opposite sides of the eddy, producing the sound waves, cancel at large distances. The M^5 dependence of the acoustic emission [see Eq. (45)] occurs because the quadrupole source is dominant, i.e. at high frequencies the highest presented multipole term dominates [see Eq. (41)], while as ω approaches the critical frequency ω_{ac} all multipole orders contribute equally if characteristic
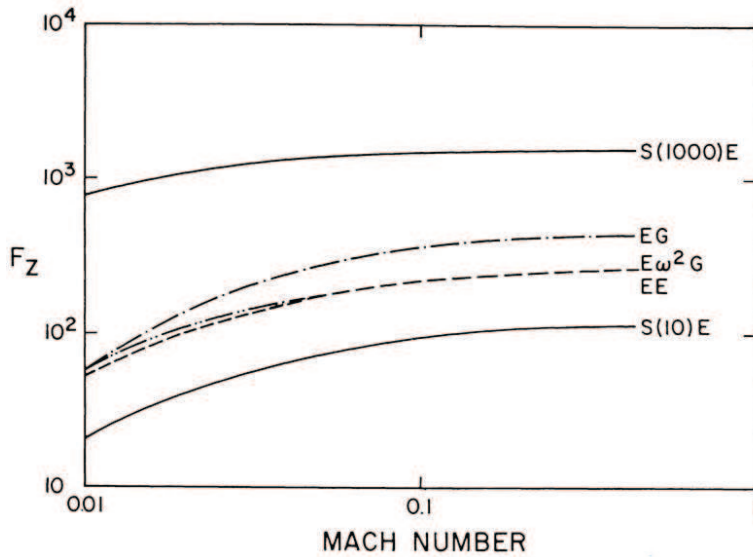
Figure 9: Total upward dimensionless gravity-wave flux (in units of $\rho_0 v^3 / l$ for $l = H$).

lengthscale of energy containing turbulent eddies is comparable to the scale hight (see Fig. 10). In addition, the largest contribution to the power comes from the high-frequency region of the spectrum, since the quadrupole emission goes as ω^4 near the cutoff frequency.

Stratification causes following effects: The power output at very small Mach numbers is less than that given by the M^5 factor. It occurs because there is a maximum frequency emitted by the turbulence, while the minimum frequency ω_{ac} increases as M^{-1}, cutting off the emission on the low side (Fig. 8). The decrease in the power output at Mach numbers approaching one, on the other hand, is due to interference. As the turbulence velocity approaches the sound speed, the wavelength of the high-frequency waves becomes much less than the size of the dominant eddies:

$$k_{wave} \approx M\omega' k_{turb}, \tag{47}$$

and the eddy, which by definition is a coherent source will interfere with the waves.

Stratification effects are small for $\omega \gg \omega_{ac}$ and at high frequencies the emission is isotropic. At frequencies near ω_b the inverse powers of $(\omega^2 - \omega_b^2 \cos^2 \theta)$

in Eq. (41) produce strong peaking of the vertical direction and the dipole and monopole-source terms become important. There is also a peak in the emission for $\omega \approx \omega_b$ due to the inverse factor $(\omega^2 - \omega_b^2)$ which becomes small if ω_{ac} is close to ω_b (Kato 1966).

Gravity wave emission occurs close to the critical angle $\theta_c = \cos^{-1} \omega/\omega_b$ because these waves propagate in that direction, where the gravitational restoring force ($\propto \omega_b^2 \cos^2 \theta$) balances the acceleration ($\propto \omega^2$). The additional restoring force enables the acceleration to be balanced at angles greater than the critical angle.

The singularity at the critical angle [see Eq. (39)] is responsible for the great efficiency of gravity wave generation. The flux does not, however, actually become infinite, because as the critical angle is approached the wave number becomes very large and the turbulence spectrum goes to zero. Thus the maximum emission of gravity waves occurs at angles very close to, but slightly greater than the critical angle.

The upward gravity wave flux emission depends on the Mach number and ratio of length scale to scale hight. It is proportional to l/H^5, rather than M^5 as for the acoustic emission, so the emission from large eddies is very strong.

In the Sun where characteristic lengthscale of the energy containing eddies is comparable to the scale height, the gravity-wave emission from turbulence in stable layers is much larger than the acoustic emission and the week-emission theory does not apply. The non-linear interaction between the waves and the turbulence must be considered.

1.4 Wave generation by turbulent convection. Solar p-Modes

Stein's (1967) problem of acoustic and gravity wave generation by turbulence in isothermal stratified atmosphere, introduced in the previous section, was extended by Goldreich and Kumar (1990) to study common process of wave
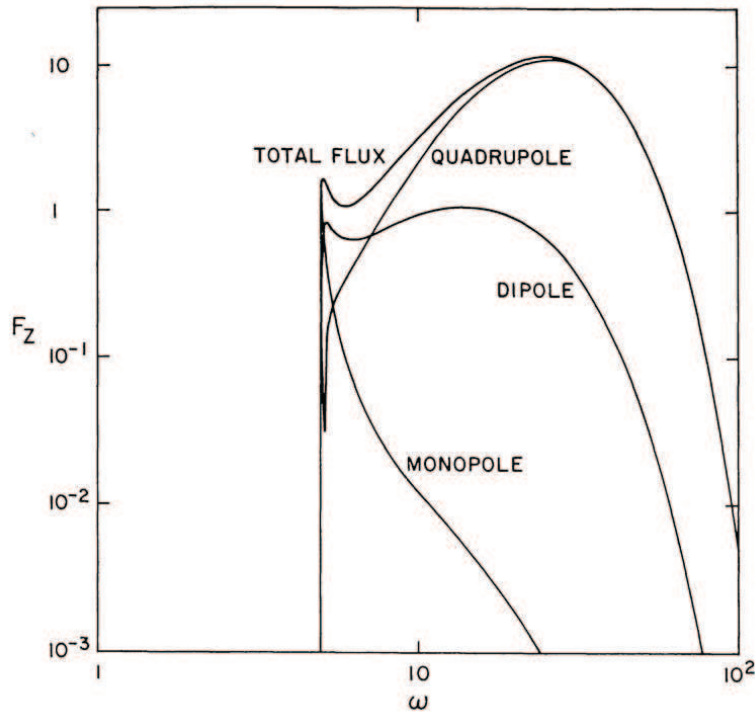
Figure 10: Spectrum of non-dimensional upward flux showing contribution of different multipole source terms, for an exponential turbulence spectrum, at Mach number 0.1.

emission by turbulent convection in stellar and planetary atmospheres. Wave emission by turbulent convection is known to play significant role is the heating of stellar chromospheres and coronas.

Goldreich and Kumar (1990) studied acoustic and gravity wave generation by turbulent convection in a plane-parallel, stratified atmosphere that consist of two semi-infinite layers, the lower adiabatic and the upper isothermal. They estimated efficiencies for the conversion of the convective energy flux into both trapped and propagating waves and calculated the total emissivities for the different wave types. Their theoretical results obtained for the amplitudes and linewidths of the solar p-Modes (trapped acoustic waves) match the observational ones in the upper part of the solar convection zone. This agreement supports the hypothesis that the solar p-Modes are stochastically excited by turbulent convection.

1.4.1 Model atmosphere and wave types

Goldreich and Kumar (1990) considered the the plane parallel atmosphere that sits in a constant gravitational field, **g**, and consists of two semi-infinite layers, the lower adiabatic and polytropic and the upper isothermal. The pressure, p, density, ρ, and temperature, T, are continuous across the interface between these layers. In the adiabatic layer

$$\Gamma = 1 + \frac{1}{m},\tag{48}$$

where Γ and m are the adiabatic and polytropic indices, respectively.

The z coordinate measures depth below the level at which the adiabatic layer would terminate in the absence of the isothermal layer.

In the polytropic adiabatic layer:

$$p = p_t\left(\frac{z}{z_t}\right)^{m+1}, \quad \rho = \rho_t\left(\frac{z}{z_t}\right)^{m}, \quad T = T_t\left(\frac{z}{z_t}\right),\tag{49}$$

where the quantities evaluated at the top of the adiabatic layer are denoted by a subscript t. The sound speed is $c_s^2 = gz/m$ and the pressure scale height is $H = z/(m+1)$.

In the isothermal layer

$$T = T_i, \quad c_s = c_{si}, \quad H = H_i, \quad p = p_i \exp(z/H_i), \quad \rho = \rho_i \exp(z/H_i),\tag{50}$$

where the parameters are distinguished by a subscript i.

The linear wave equations, in terms of the variable $Q \equiv p_1/\rho$ (Eulerian enthalpy perturbations) are as follows:

$$\frac{d^2Q}{dz^2} + \frac{m}{z}\frac{dQ}{dz} + \left(\frac{\omega^2}{c_s^2} - k_h^2\right)Q = 0,\tag{51}$$

in the adiabatic layer, and

$$\frac{d^2Q}{dz^2} + \frac{1}{H_i}\frac{dQ}{dz} + \left[\frac{\omega^2}{c_{si}^2} - k_h^2\left(1 - \frac{\omega_b^2}{\omega^2}\right)\right]Q = 0, \tag{52}$$

in the isothermal layer (Kumar and Goldreich 1989). Here ω is the wave frequency and $\mathbf{k}_h$ is the horizontal wavevector.

The normal modes are obtained by solving Eqs. (51) and (52) subject to $Q \to 0$ as $z \to \infty$, Q continuous across the interface at z_t and the appropriate boundary conditions as $z \to -\infty$.

The modes are classified as trapped or propagating, and as composed of acoustic or gravity waves. The adiabatic layer supports acoustic waves, but not gravity waves and it refracts acoustic waves upward. Thus, propagating modes must be traveling waves in the isothermal atmosphere.

Solutions of the wave equation in the isothermal atmosphere (52) are proportional to $\exp(-k_\pm z)$, where

$$k_\pm = \left\{\frac{1}{2H_i} \pm i\sqrt{\left[\left(\frac{\omega}{\omega_{ac}}\right)^2 - 1\right]\frac{1}{(2H_i)^2} + \left[\left(\frac{\omega_b}{\omega}\right)^2 - 1\right]k_h^2}\right\}. \tag{53}$$

Here

$$\omega_{ac}^2 = \frac{\gamma g}{4H_i} \tag{54}$$

is the acoustic cutoff frequency and

$$\omega_b^2 = \frac{(\gamma - 1)g}{\gamma H_i} \tag{55}$$

is the Brunt-Väisälä frequency.

For $2k_h H_i \ll 1$ there are two types of traveling waves in the isothermal atmosphere: a high frequency acoustic wave with $\omega > \omega_{ac}$ and a low frequency gravity wave with $\omega < 2k_h H_i \omega_b$.

The dispersion relation for trapped modes that correspond to evanescent solutions in the isothermal layer reads:

$$\omega^2 = \frac{2}{m} g k_h \left(n + \frac{m}{2} \right), \tag{56}$$

where the integer n denotes the number of nodes in the radial displacement eigenfunction (Christensen-Dalsgaard 1980; Christensen-Dalsgaard and Gough 1980) and, thus, these modes are restricted to a discrete set of eigenfrequencies for fixed k_h.

Trapped acoustic modes, or p-Modes, correspond to $n \neq 0$. Modes with $n = 0$ are surface gravity waves, or f-Modes. Trapped gravity waves, or g-Modes with $n \neq 0$ do not exist since the adiabatic layer is neutrally stratified and its Brunt-Väisälä frequency vanishes.

For modes with $2 k_h H_i \ll 1$ the solution of wave equation satisfies the normalization condition:

$$I \approx \int_{z_t}^{\infty} dz \frac{\rho}{c_s^2} Q_\omega Q^*_{\omega'} = \delta_{\omega,\omega'}, \tag{57}$$

where Eq. (51) is used, because the most of the contribution to the energy integral comes from the adiabatic layer. For $\omega = \omega'$, this integral evaluates the potential energy of a trapped mode in the adiabatic layer.

1.4.2 Wave modes excitation by turbulent convection. Source terms

Turbulent convection adds monopole, dipole and quadrupole source terms to the linear wave equation (51) for the adiabatic layer. These sources appear from the expansion and contraction of fluid due to the gain and loss of specific entropy, buoyancy force variations associated with these entropy changes, and momentum transport by the fluctuating Reynold's stress.

From following linearized equations for mass and momentum conservation and equation of state for a perfect adiabatic gas with the isentropic background state:

$$\frac{\partial \rho_1}{\partial t} + \nabla \cdot (\rho \mathbf{v}) = 0, \tag{58}$$

$$\frac{\partial \rho_1 \mathbf{v}}{\partial t} + \nabla p_1 - \rho_1 \mathbf{g} = -\nabla \cdot (\rho \mathbf{v} \mathbf{v}) \equiv \mathcal{F}, \tag{59}$$

and

$$\frac{p_1}{p} - \frac{\Gamma \rho_1}{\rho} = \frac{s}{c_v}, \tag{60}$$

where $\rho_1, p_1, \mathbf{v}$ and s are the Eulerian density, pressure, velocity and entropy perturbations associated with the turbulent convection and the waves it generates, after standard manipulations one can obtain the inhomogeneous wave equation:

$$\nabla^2 Q + \frac{g}{c_s^2}\frac{\partial Q}{\partial z} - \frac{1}{c_s^2}\frac{\partial^2 Q}{\partial t^2} = \frac{S^{(1)} + S^{(2)}}{\rho}, \tag{61}$$

where

$$S^{(1)} = -\rho \frac{\partial^2}{\partial t^2}\left(\frac{s}{c_p}\right) - g\frac{\partial}{\partial z}\left(\frac{\rho s}{c_p}\right), \tag{62}$$

$$S^{(2)} = \nabla \cdot \mathcal{F}. \tag{63}$$

The first term in $S^{(1)}$ arises from the fluid volume change due to the entropy change at fixed pressure and it is a monopole source. The second term is a dipole source. It reflects the buoyancy force variations associated with this volume change and involves a variation of the density of momentum supplied by the external gravitational force. The double divergence of the Reynolds stress in $S^{(2)}$ reflects the redistribution of momentum by internal stresses. It is a quadrupole source.

Provided we drop the term $c_s^{-2}\partial^2 Q/\partial t^2$ on the left-side of (61) as a first approximation in the limit of subsonic turbulence, then this equation determines

the near field turbulent pressure perturbations from the turbulent velocity and entropy perturbations. The term $c_s^{-2}\partial^2 Q/\partial t^2$ connects the near field perturbations to the wave field perturbations.

The total enthalpy perturbation, $Q(x,t)$, is expanded in terms of the normal modes, $Q_\alpha(z)$, as

$$Q = \frac{1}{\sqrt{2\mathcal{A}}}\sum_a \left[A_\alpha Q_\alpha \exp\left(-i\omega t + i\mathbf{k}_h \cdot \mathbf{x}\right) + A_\alpha^* Q_\alpha^* \exp\left(i\omega t - i\mathbf{k}_h \cdot \mathbf{x}\right)\right], \quad (64)$$

where $\mathcal{A}$ is the horizontal cross section of the atmosphere and $A_\alpha(t)$ are slowly varying functions of time, $|dA_\alpha/dt| \ll \omega|A_\alpha|$. After some algebra and using the approximation $k_h|Q_\alpha| \leq |\partial Q_\alpha/\partial z|$, which is valid near the top of the adiabatic layer, Eqs. (61), (64) and (51) give the following expressions:

$$A_\alpha^{(1)}(t) \approx -\frac{1}{2i\omega\mathcal{A}^{1/2}}\int_{-\infty}^t dt \int d^3x \frac{\rho c_s^2 s}{c_p}\frac{\partial^2 Q_\alpha^*}{\partial z^2}\exp\left(i\omega t - i\mathbf{k}_h \cdot \mathbf{x}\right), \quad (65)$$

and

$$A_\alpha^{(2)}(t) \approx \frac{1}{2i\omega\mathcal{A}^{1/2}}\int_{-\infty}^t dt \int d^3x \rho v_z^2 \frac{\partial^2 Q_\alpha^*}{\partial z^2}\exp\left(i\omega t - i\mathbf{k}_h \cdot \mathbf{x}\right), \quad (66)$$

which provide order of magnitude estimates for $A_\alpha^{(1)}(t)$ and $A_\alpha^{(2)}(t)$. The lower limit $-\infty$ in the integral over t involves the assumption that damping erases the memory of excitations from the distant past.

The monopole and dipole terms in $S^{(1)}$ produce more acoustic radiation than the quadrupole term in $S^{(2)}$. However Goldreich and Kumar (1990) compared the relative sizes of $A_\alpha^{(1)}(t)$ and $A_\alpha^{(2)}(t)$ both for energy bearing and inertial range eddies and demonstrated that destructive interference between monopole and dipole radiation fields holds the acoustic emissivity of turbulent convection at the level characteristic of free turbulence (turbulence without external forces) for which the emissivity is dominated by acoustic quadrupoles. They used the Eq. (66) for quadrupole emission to calculate the rate at which turbulent

convection pumps energy into the different wave modes using the assumption that different eddies of similar size are uncorrelated.

For the excitation rate of the mode α calculations yield that $\dot{E}_\alpha$ is dominated by contribution from $z \sim z_*$ for all wave modes, where z_* corresponds to the layer where the turnover time of the energy bearing eddies is most equal to the mode period and:

$$\dot{E}_\alpha \sim \frac{\rho_t^2 H_t^8}{\tau_t} \frac{1}{(\omega\tau_t)^{(5m+21)/(m+3)}\left[1 + (\omega\tau_t)^{3(3m+5)/2(m+3)}\right]}\left|\frac{\partial^2 Q_\alpha(z_*)}{\partial z^2}\right|^2, \qquad (67)$$

where

$$u_* \sim 1 + \frac{1}{(\omega\tau_t)^{3/(m+3)}} \qquad (68)$$

and $\tau_t \sim 1/(M_t\omega_{ac})$ is the characteristic time scale of the energy bearing eddies at the top of the convection zone.

1.4.3   P-Modes

P-Mode is a standing acoustic wave trapped between an upper reflecting layer at z_1, where $\omega/c_s(z_1) = 1/2H(z_1)$, and a lower turning point at z_2, where $\omega/c_s(z_2) = k_h$. For $z > z_1$ and $z < z_2$ the mode is evanescent. In the region of propagation $z_1 \ll z \ll z_2$ the approximate WKB solution of Eq. (51) in the dual limit $\omega \ll \omega_{ac}$ and $2k_h H_t \ll 1$ is as follows:

$$Q \sim \left(\frac{z_t}{z}\right)^{(m-1)/2} B_p \sin\left[2\omega\left(\frac{mz}{g}\right)^{1/2} + \phi_p\right], \qquad (69)$$

where B_p is determined from the normalization equation (57) and boundary conditions. The result is given by

$$B_p^2 \sim \frac{z_t^m \omega^{2(m-1)} k_h}{g^{(m-2)}\rho_t}. \qquad (70)$$

From Eqs. (69) and (70) we can estimate $\partial^2 Q / \partial z^2$:

$$\frac{\partial^2 Q}{\partial z^2} \sim \left(\frac{\omega^2}{g}\right)^2 B_p, \tag{71}$$

for $z_t \leq z \ll z_1$.

The excitation rate for p-Modes can be obtained from Eqs. (67) and (71):

$$\dot{E}_p \sim \rho_t H_t^3 v_t^3 M_t^{2(m+2)} k_h \frac{(\omega \tau_t)^{(2m^2+7m-3)/(m+3)}}{1 + (\omega \tau_t)^{3(3m+5)/2(m+3)}}. \tag{72}$$

At fixed k_h, $\dot{E}_p$ varies as $\omega^{(2m^2+7m-3)/(m+3)}$ for $\omega \tau_t < 1$ and as $\omega^{(4m-7)/2}$ for $\omega \tau_t > 1$.

For the energy input rate per mode along the (nth) p-Mode ridge, the Eqs. (72) and (56) yield:

$$\dot{E}_p \sim \frac{\rho_t H_t^2 v_t^3 M_t^{2(m+3)}}{(n+m/2)} \frac{(\omega \tau_t)^{(2m^2+9m+3)/(m+3)}}{1 + (\omega \tau_t)^{3(3m+5)/2(m+3)}} \tag{73}$$

The total flux of energy going into p-Mode is:

$$F_p = \frac{1}{\mathcal{A}} \sum_p \dot{E}_p = \frac{1}{2\pi} \sum_n \int dk_h k_h \dot{E}_p \sim \rho_t v_t^3 M_t^{15/2}, \tag{74}$$

where the sum over p includes all p-Modes, the sum over n includes all p-Mode dispersion ridges and $\int dk_h$ is over all modes along a ridge.

Eq. (73) shows that for $\omega \tau_t \gg 1$ the energy input rate is proportional to $(\omega \tau_t)^{(4m-3)/2}$, which increases with increasing ω for $m > \frac{3}{4}$. Since the maximum frequency for trapped p-Modes is ω_{ac}, most of the energy flux goes into modes whose frequencies lie just below the acoustic cutoff, $\omega \leq \omega_{ac}$, and is emitted by inertial range eddies with $h \sim M_t^{3/2} H_t$, located in the top scale height of the convection zone.

1.4.4 Solar p-Modes

Eq. (72) shows that the power input to individual p-Modes $\dot{E}_p$ varies as $\omega^{(2m^2+7m-3)/(m+3)}$ at frequencies $\omega \ll v_t/H_t$. Libbrecht (1988) has determined $\dot{E}_p(\omega)$ from his solar p-Mode observations and found that the amplitudes and linewidths of the solar p-Modes imply $\dot{E}_p \propto \omega^8$ for $\omega \ll 2 \times 10^{-2} s^{-1}$. The theoretical exponent obtained by Goldreich and Kumar (1990) is in agreement with the observational result for $m \approx 4$, the polytropic index that is obtained from the density profile in the upper part of the solar convection zone (the hydrogen ionization zone). This agreement supports the hypothesis that the solar p-Modes are stochastically excited by turbulent convection.

For $\omega \gg 2 \times 10^{-2} s^{-1}$ Libbrecht (1988) found $\dot{E}_p \propto \omega^{-5}$, while the Eq. (72) gives $\dot{E}_p \propto \omega^{(4m-7)/2}$ for $\omega \gg v_t/H_t$, or $\dot{E}_p \propto \omega^{4.5}$ for $m = 4$. This failure of the theoretical result is due to the ignorance of the modification of the eigenfunctions in the polytropic layer for ω close to ω_{ac} by the boundary conditions imposed at the interface with the isothermal layer.

1.4.5 Generation of trapped and propagating waves

Goldreich and Kumar (1990) found that wave generation is concentrated at the top of the convection zone, where the turbulent Mach number $M_t = v_H/c_s$ peaks. They assumed $M_t \ll 1$ and calculated the dimensionless efficiency, η, for the conversion of the convective energy flux into the wave energy flux to be $\eta \sim M_t^{15/2}$ for p-Modes, f-Modes (gravity waves confined near the surface of the convection zone) and propagating acoustic waves, and $\eta \sim M_t$ for propagating gravity waves. Most of the energy going into p-Modes, f-Modes and propagating acoustic waves is emitted by inertial range eddies of size $h \sim M_t^{3/2} H_t$ at $\omega \sim \omega_{ac}$ and $k_h \sim 1/H_t$. The energy emission into propagating gravity waves is dominated by energy bearing eddies of size $\sim H_t$ and is concentrated at $\omega \sim$

$v_t/H_t \sim M_t \omega_{ac}$ and $k_h \sim 1/H_t$.

1.5 Discussion and summary

Lighthill's acoustic analogy represents an approximation of fully nonlinear problem and is taken to be analogous to the problem of sound propagating in a linear acoustic medium at rest subject to an external forcing that represents the turbulent source. Lighthill reformulated the Navier-Stokes equation into an exact, inhomogeneous wave equation whose source terms are important only within the turbulent region. Sound is expected to be such a very small component of the whole motion that, once generated, its back-reaction on the source region can be neglected.

Goldstein (2002) rewrote the the Navier-Stokes equations into the general set of linearized inhomogeneous Euler equations (in convective form) but with modified dependent variables. His method put the classical approaches to the jet noise problem on a more rational basis and also extended in new directions. Formulation of the generalized acoustic analogy (Goldstein 2002) implies: (i) dividing the flow variables into their mean and fluctuating parts; (ii) subtracting out the equation for the mean flow; (iii) collecting all the linear terms on one side of equations and the nonlinear terms on the other side; (iv) treating the latter terms as the known terms of sound.

Various experiments and numerical simulations (Whitmire and Sarkar 2000; Seror *et al.* 2001; Freund 2003; Panickar *et al.* 2005 and references therein) verify the ability of the Lighthill acoustic analogy to predict sound generated by a three-dimensional turbulent source containing many length and time scales. This studies are based on combined analytical-modeling approach: the turbulence is computed using a method such as DNS (direct numerical simulation) or LES (large eddy simulation), and the far filed sound is calculated using an acoustic analogy.

Stein (1967) extended Lighthill's method to calculate the acoustic and gravity-wave emission by turbulent motions in solar convective zone, where the characteristic size of energy containing turbulent eddies is considered to be comparable to the scale height of the stratification produced by gravity. His calculations show, that stratification cuts off the acoustic radiation at low Mach numbers. Form typical solar parameters gravity wave generation was found to be much more efficient than acoustic radiation.

Goldreich and Kumar (1990) studied acoustic and gravity wave generation by turbulent convection in more realistic model atmosphere and estimated efficiencies for the conversion of the convective energy flux into both trapped and propagating waves. Their theoretical results obtained for the amplitudes and linewidths of the solar p-Modes match the observational ones in the upper part of the solar convection zone. This agreement supports the hypothesis that the solar p-Modes are stochastically excited by turbulent convection.

2 Infrasound generation by tornadic storms

Recent observations of infrasound originating from regions of severe weather show that infrasound dominant frequency occurs in a passband from 0,5 to 2,5 Hz, with peak frequencies between 0,5 and 1 Hz (e.g. Bedard 2005; Bedard *et al.* 2004a). Analyzing acoustic radiation from severe thunderstorms, Bedard (2004a) concluded that radiation of infrasound in this passband is not a natural consequence of all severe weather. Infrasound of a tornadic thunderstorm is much stronger than infrasound of a nonsevere weather system and therefore, mesocyclones or tornadoes may be a primary mechanism for infrasound production in this frequency range (Szoke *et al.* 2004).

Detection of infrasound appears to have significant potential for improving tornado forecasting. The acoustic power radiated by strong convective storm system could be as high as 10^7 watts (Georges 1988) and infrasound below 1 Hz can travel for distances of thousands of kilometers from a source without significant absorption.

Over the years, several potential sound generation mechanisms were compared with measured characteristics of infrasound (Georges and Greene 1975; Georges 1988; Bedard and Georges 2000; Beasley *et al.* 1976). Such mechanisms include release of latent heat, dipole radiators, boundary layer turbulence, lightning, electrostatic sources and vortex sound (radial vibrations and the co-rotation of suction vortices). Georges (1976) eliminated many sources as likely candidates and concluded that vortex sound was the most likely model. Bedard (2005) also found that the radial vibration model (Abdullah 1966) is most consistent with infrasonic data. This model predicts that the fundamental frequency of radial vibration will be inversely proportional to core radius. A radius of about 200 m will produce a frequency of 1 Hz. Schecter *et al.* (2008) performed numerical simulation of the adiabatic generation of infrasound by tornadoes and also simulated the infrasound radiated from a

single-cell non-tornadic thunderstorm in a shear-free environment, using Regional Atmospheric Modeling System (RAMS). In the latter simulation dominant infrasound in the $0.1 - 10$ Hz frequency band, so called "thunderstorm noise" appeared to radiate from the vicinity of the melting level, where diabatic processes involving hail were active. They found that 3D Rossby waves of a tornado-like vortices can generate stronger $0.1 - 10$ Hz infrasound at or above the simulated non-tornadic thunderstorm noise if maximum wind speed of the vortex exceeds a modest threshold.

Georges and Green (1975) noted that infrasound often precedes an observed tornado by up to an hour. Many other case studies of infrasound associated with tornadoes and tornadic storms (Bedard *et al.* 2004a; Bedard *et al.* 2004b) are consistent with this result. Bedard *et al.* (2004b) analyzed all significant infrasonic signals data collected in 2003 during the continuous Infrasonic Network (ISNeT) operation. Summarizing differences between predicted acoustic signal arrival times from reported tornados and start times of infrasonic detection they concluded that infrasound is usually produced substantially before (0.5 - 1 hrs) reports of tornadoes and that there could be other sound generation processes active not related to tornadic vortices. Bedard *et al.* (2004b) also indicated the difference between the infrasonic bearing sectors and the vortex location and concluded that, although the storm environment wind and temperature gradient could be responsible for bearing deviations, there remains the possibility that another storm feature could radiate infrasound from another location within the storm (bedard 2004).

Broad and smooth spectra of observed infrasound radiation indicates that turbulence is a promising sources of the radiation. Acoustic radiation from turbulent convection was studied by Akhalkatsi and Gogoberidze (2009) taking into account effects of stratification, temperature fluctuations and moisture of air, using Lighthill's acoustic analogy. It was shown for typical parameters of strong convective storms, infrasound radiation should be dominated by a

monopole acoustic source related to the moisture of the air. The total power of this source is two orders higher than thermo-acoustic and Lighthill's quadrupole radiation power, being of order 10^7 watts, in qualitative agreement with observations of strong convective storms (Bowman and Bedard 1971; Bedard and Georges 2000; Georges and Greene 1975; Georges 1973).

In this chapter we study acoustic radiation from turbulent convection using Lighthill's acoustic analogy and taking into account the effects of stratification, temperature fluctuations and moisture in the air. Formulation of the generalized acoustic analogy (Goldstein 2002) implies: (i) dividing the flow variables into their mean and fluctuating parts; (ii) subtracting out the equation for the mean flow; (iii) collecting all the linear terms on one side of equations and the nonlinear terms on the other side; (iv) treating the latter terms as the known terms of sound.

We show that in saturated moist air turbulence in addition to the Lighthill's quadrupole and known dipole sources of sound (related to stratification and temperature fluctuations) there exist monopole sources related to heat and mass production during the condensation of moisture. It appears that infrasound radiation from convective storms should be dominated by acoustic monopole sources related to the moisture in the air. We show that for typical parameters of strong convective storms the acoustic output of this monopole source is two orders of magnitude stronger than Lighthill's quadrupole source, whereas the dipole radiation related to temperature inhomogeneities is of the same order as radiation of Lighthill's quadrupole source. The dipole source related to stratification and the dipole and quadrupole sources related to inhomogeneity of background velocity are inefficient sources of sound. The total power of the source related to moisture is of order 10^7 watts for typical parameters of strong convective storms, in qualitative agreement with observations (Gossard and Hooke 1975; Bedard and Georges 2000; Georges and Greene 1975; Georges 1973).

The section is organized as follows: In subsection 2.1 equations governing the sound generation by turbulence for a moist atmosphere are obtained in the framework of Lighthill's acoustic analogy. Various sources of acoustic radiation are analyzed in subsection 2.2. An application of the results to infrasound generation in strong convective storms is made in subsection 2.3. Conclusions are given in subsection 2.4.

2.1 General formalism

The dynamics of the convective motion of moist air is governed by the continuity, Euler, heat, humidity and ideal gas state equations:

$$\frac{D\rho}{Dt} + \rho\nabla\cdot\mathbf{v} = 0, \tag{75}$$

$$\rho\frac{D\mathbf{v}}{Dt} + 2\rho\mathbf{\Omega}\times\mathbf{v} = -\nabla p - \rho\nabla\Phi, \tag{76}$$

$$T\frac{Ds}{Dt} = -L_\nu\frac{Dq}{Dt}, \tag{77}$$

$$\rho = \frac{p}{RT}\frac{1}{1-q+q/\epsilon} = \frac{p}{RT}\frac{1}{1+aq}, \tag{78}$$

where $\mathbf{v}$, $2\mathbf{\Omega}\times\mathbf{v}$, ρ and p are velocity, Coriolis acceleration, density and pressure respectively; $D/Dt \equiv \partial/\partial t + \mathbf{v}\cdot\nabla$ is Lagrangian time derivative; L_ν is the latent heat of condensation and q is the mass mixing ratio of water vapor (humidity mixing ratio)

$$q \equiv \frac{\rho_\nu}{\rho}, \tag{79}$$

where ρ_ν is the mass of water vapor in unit volume; $\epsilon \equiv m_\nu/m_d \approx 0.622$ is the ratio of molecular masses of water and air; $a = 0.608$ and R is the universal gas constant.

In the set of Eqs. (75)-(78) diffusion and viscosity effects are neglected due to the fact that they have a minor influence on low frequency acoustic wave generation and propagation.

In this analysis we also assume $\Omega = 0$, as it is well known (Bluestein 1992) that Coriolis effects are negligible for mesoscale convective system dynamics. On the other hand, when the frequency of acoustic waves (Ω_a) satisfy the condition $\Omega_a \gg \Omega$, Coriolis effects also have negligible influence on acoustic wave dynamics.

The main idea of Lighthill's acoustic analogy is reformulation of the governing equations in a form suitable for the study of acoustic wave radiation process. To proceed in this direction one has to choose an appropriate "acoustic variable", that describes acoustic waves in the irrotational regions of the fluid. The generalized Bernoulli's theorem (Batchelor 1967) suggests that the total enthalpy

$$B \equiv E + \frac{p}{\rho} + \frac{v^2}{2} + \Phi, \tag{80}$$

where Φ is gravitational potential energy per unit mass, E is internal energy and $\nabla\Phi \equiv -\mathbf{g}$, is one of the possible appropriate choices (Howe 2001). B is constant in a steady irrotational flow and at large distances from acoustic sources perturbations of B represent acoustic waves.

To derive the acoustic analogy equation in terms of the total enthalpy it is useful to rewrite Euler's equation in the Crocco's form as follows

$$\rho\frac{D\mathbf{v}}{Dt} + \nabla B = -\omega \times \mathbf{v} + T\nabla s, \tag{81}$$

where ω is vorticity, T is temperature, s is specific entropy and

$$Tds = dE + pd\left(\frac{1}{\rho}\right) = dB - \frac{dp}{\rho} - d\Phi - d\left(\frac{v^2}{2}\right). \tag{82}$$

From the thermodynamic identity

$$d\rho = \left(\frac{\partial \rho}{\partial p}\right)_{s,q} dp + \left(\frac{\partial \rho}{\partial s}\right)_{p,q} ds + \left(\frac{\partial \rho}{\partial q}\right)_{s,p} dq, \tag{83}$$

where the subscripts serve as the reminders of the variables held constant, using Eqs. (78) we obtain

$$d\rho = \frac{1}{c_s^2} dp - \frac{\rho}{c_p} ds + \frac{a\rho}{1 + aq} dq, \tag{84}$$

where

$$c_s \equiv \left(\frac{\partial p}{\partial \rho}\right)_{s,q}^{1/2}, \tag{85}$$

is the sound velocity and

$$c_p \equiv T \left(\frac{\partial s}{\partial T}\right)_{p,q} \tag{86}$$

is the specific heat of the air.

Eliminating the convective derivative of the density from Eq. (75) using Eq. (84) we have that

$$\frac{1}{\rho c_s^2}\frac{Dp}{Dt} + \nabla \cdot \mathbf{v} = \frac{1}{c_p}\frac{Ds}{Dt} + \frac{1}{1+aq}\frac{Dq}{Dt}. \tag{87}$$

Subtracting the divergence of Eq. (81) from the time derivative of Eq. (87) and using Eq (77) after long but straightforward calculations we obtain

$$\left(\frac{D}{Dt}\left(\frac{1}{c_s^2}\frac{D}{Dt}\right) - \frac{\nabla p \cdot \nabla}{\rho c_s^2} - \nabla^2\right) B = $$
$$S_L + S_T + S_q + S_m + S_\gamma, \tag{88}$$

where $\gamma \equiv c_p/c_v$ is the ratio of specific heats and

$$S_L \equiv \left(\nabla + \frac{\nabla p}{\rho c_s^2}\right) \cdot (\omega \times \mathbf{v}), \tag{89}$$

$$S_T \equiv -\left(\nabla + \frac{\nabla p}{\rho c_s^2}\right) \cdot (T\nabla s), \tag{90}$$

$$S_q \equiv \frac{\partial}{\partial t}\left(\frac{\gamma T}{c_s^2}\frac{Ds}{Dt}\right) + (\mathbf{v}\cdot\nabla)\left(\frac{T}{c_s^2}\frac{Ds}{Dt}\right), \tag{91}$$

$$S_m \equiv \frac{\partial}{\partial t}\left(\frac{a}{1+aq}\frac{Dq}{Dt}\right), \tag{92}$$

$$S_\gamma \equiv p\frac{\partial\gamma}{\partial q}\left(\frac{\partial q}{\partial t}(\mathbf{v}\nabla)p - \frac{\partial p}{\partial t}(\mathbf{v}\nabla)q\right). \tag{93}$$

Eq. (88) is suitable for the identification of different acoustic sources and the study of their acoustic output.

The nonlinear wave operator on the left of Eq. (88) is identical with that governing the propagation of sound in an irrotational, homentropic flow. Therefore the terms on the right may be identified as acoustic sources. Propagation of infrasound in the atmosphere was intensively studied by different authors (Ostashev *et al.* 2001) and references therein) and will not be considered in this paper.

To further simplify the analysis of the acoustic output of different sources we make several standard assumptions:

(a) For acoustic wave generation process at low Mach number flow, all the convective derivatives in Eq. (88) can be replaced by time derivatives $\partial/\partial t$ (Goldstein 1976);

(b) For acoustic waves with the wavelength λ not exceeding the stratification length scale

$$\lambda \leq H \equiv \frac{c_s^2}{g} \approx 10^4\text{m}, \tag{94}$$

one can also neglect the influence of stratification on the acoustic wave generation process and consider background thermodynamic parameters in Eq. (88) as constants (Stein 1967).

(c) Neglecting nonlinear effects of acoustic wave propagation and scattering of sound by vorticity and taking into account that $M \ll 1$, for the acoustic pressure in the far field we have

$$p'(\mathbf{x}, t) \approx \rho_0 B(\mathbf{x}, t). \qquad (95)$$

(d) Eq. (88) is equivalent to initial set of Eqs. (75)-(78) and therefore it describes not only acoustic waves, but also the instability wave solutions that are usually associated with large scale turbulent structures and continuous spectrum solutions related to "fine-grained" turbulent motions (Goldstein 2002; Goldstein 1984). In the presence of any kind of inhomogeneity, such as stratification or velocity shear, linear coupling between these perturbations is possible, and in principle acoustic waves can be generated by both instability waves and continuous spectrum perturbations. But in the case of low Mach number ($M \ll 1$) flows both kinds of perturbations are very inefficient sources of sound. The acoustic power is proportional to $e^{-1/2M^2}$ and $e^{-\pi\delta/2M}$ for instability waves and continuous spectrum perturbations respectively (Crighton and Huerre 1990). In the last expression δ is the ratio of length scales of energy containing vortices and background velocity inhomogeneity ($V/\partial_z V$). In the case of supercell thunderstorms $M \sim 0.1 - 0.15$ and $\delta \sim 10^{-2}$, therefore both linear mechanisms have negligible acoustic output and attention should be payed to sources of sound related to nonlinear terms and entropy fluctuations that will be studied next.

With these assumptions Eq. (88) simplifies and reduces to

$$\frac{1}{\rho_0} \left(\frac{1}{c_s^2} \frac{\partial^2}{\partial t^2} - \nabla^2 \right) p' = S_L + S_T + S_\gamma + S_q + S_m, \tag{96}$$

with

$$S_L \approx \nabla \cdot (\omega \times \mathbf{v}), \tag{97}$$

$$S_T \approx -\nabla \cdot (T \nabla s), \tag{98}$$

$$S_\gamma = p \frac{\partial \gamma}{\partial q} \left(\frac{\partial q}{\partial t} (\mathbf{v} \nabla) p - \frac{\partial p}{\partial t} (\mathbf{v} \nabla) q \right). \tag{99}$$

$$S_m \approx \frac{a}{1 + aq} \frac{\partial^2 q}{\partial t^2}, \tag{100}$$

$$S_q \approx -\frac{\gamma L_\nu}{c_s^2} \frac{\partial^2 q}{\partial t^2}, \tag{101}$$

The first three terms on the right hand side of Eq. (96) represent well known sources of sound: the first term represents Lighthill's quadrupole source (Lighthill 1952); the second term is a dipole source related to temperature fluctuations (Goldstein 1976); S_γ is a monopole source related to variability of adiabatic index, that usually have negligible acoustic output (Howe 2001) and will not be considered in the present section; Eq. (96) shows that in the case of saturated moist air turbulence there exist two additional sources of sound. S_q and S_m are monopole sources related to nonstationary heat and mass production during the condensation of moisture, respectively.

2.2   Analysis of different sources

For estimation of different acoustic sources we follow the standard procedure (Goldstein 1976; Howe 2001). Namely, using a free space Green function of the wave equation

$$G(t, t', \mathbf{x}, \mathbf{x}') = \frac{\delta(t - t' - |\mathbf{x} - \mathbf{x}'|/c_s)}{4\pi c_s^2 |\mathbf{x} - \mathbf{x}'|}, \tag{102}$$

acoustic pressure fluctuations corresponding to a source S_i can be written as

$$p_i'(x, t) = \frac{1}{4\pi c_s^2} \int \frac{[S_i]_{t=t_*}}{|\mathbf{x} - \mathbf{x}'|} d^3\mathbf{x}', \tag{103}$$

where $t_* = t - |\mathbf{x} - \mathbf{x}'|/c_s$.

It has to be noted that using a free space Green function we neglect the effect of the acoustic wave reflection from the ground. In general this is not correct approximation for the study of low frequency acoustic wave dynamics in the atmosphere, but because we are interested only in the total acoustic power of the atmospheric turbulence the neglect of this effect is an adequate approximation.

Calculating acoustic radiation in the far field ($|\mathbf{x}| \gg |\mathbf{x}'|$), we can use following expansions

$$|\mathbf{x} - \mathbf{x}'| \approx |\mathbf{x}| - \frac{\mathbf{x} \cdot \mathbf{x}'}{|\mathbf{x}|}, \tag{104}$$

$$S_\alpha(t_*) \approx S_\alpha\left(t - \frac{|\mathbf{x}|}{c_s}\right) + \frac{\mathbf{x} \cdot \mathbf{x}'}{c_s|\mathbf{x}|} \frac{\partial}{\partial t} S_\alpha\left(t - \frac{|\mathbf{x}|}{c_s}\right), \tag{105}$$

and using plane wave approximation for far field derivatives

$$\frac{\partial}{\partial x_i} \approx -\frac{x_i}{c_s|\mathbf{x}|} \frac{\partial}{\partial t}, \tag{106}$$

for the Lighthill source we obtain

$$p_L'(x, t) = -\frac{\rho_0 x_i x_j}{4\pi c_s^2 |\mathbf{x}|^3} \frac{\partial^2}{\partial t^2} \int v_i v_j d^3\mathbf{x}', \tag{107}$$

which corresponds to quadrupolar radiation field.

p_L' can be estimated in terms of the characteristic velocity v and length scale l of energy containing turbulent eddies. Fluctuations in $v_i v_j$ in different regions of the turbulent flow separated by distances greater then l tend to be

statistically independent, and therefore generation of sound can be considered as a collection of F/l^3 independent eddies, where F is the volume occupied by the turbulence. The dominant frequency of the motion is $\sim v/l$, so the wavelength of the radiated sound is $\lambda \sim l/M_t$, where $M_t \equiv v/c_s \ll 1$ is turbulent Mach number. Therefore, each eddy is acoustically compact. Acoustic pressure generated by single eddy is $p'_{L1} \sim (l/|\mathbf{x}|)\rho_0 v^2 M_t^2$, and the acoustic power it radiates is $N_{L1} \sim 4\pi |\mathbf{x}|^2 p'^2_{L1}/\rho_0 c_s \approx \rho_0 v^3 l^2 M_t^5$, which corresponds to Lighthill's eighth power law. For total acoustic power this yields Proudman's estimate (Proudman 1952),

$$N_L \sim \frac{\rho_0 v^8}{l c_s^5} F. \tag{108}$$

Similar arguments can be used for the estimation of the acoustic power of a thermo-acoustical source S_T related to density (and therefore temperature) fluctuations, producing a dipole source (Howe 2001). The physics of this kind of acoustic radiation is the following: "hot spots" or "entropy inhomogeneities" behave as scattering centers at which dynamic pressure fluctuations are converted directly into sound. The acoustic power is (Akhalkatsi *et al.* 2004):

$$N_T \sim \frac{\rho_0 \Delta T^2 v^6}{l T^2 c_s^3} F = \frac{\Delta T^2}{M_t^2 T^2} N_L, \tag{109}$$

where ΔT denotes the rms of temperature fluctuations.

Acoustic sources S_q and S_m are related to the moisture of the air. They produce monopole radiation and physically have the following nature: suppose there exist two saturated air parcels of unit mass with different temperatures T_1 and T_2 and water masses $m_\nu(T_1)$ and $m_\nu(T_2)$. Mixing of these parcels leads to the condensation of water due to the fact that

$$2m_\nu(T_1/2 + T_2/2) < m_\nu(T_1) + m_\nu(T_2). \tag{110}$$

The water condensation leads to two effects important for sound generation:

production of heat and decrease in the mass of the gass. Both of these effects are known to produce monopole radiation (Goldstein 1976; Howe 2001). Consequently, turbulent mixing of saturated air with different temperatures will not only lead to dipole thermo-acoustical radiation (109), but also to monopole radiation.

According to Eqs. (79) and (110) for the humidity mixing ratio fluctuation q_s' we have

$$q_s' = q_s(T + T') + q_s(T - T') - 2q_s(T). \tag{111}$$

In the limit $T'/T \ll 1$ this yields

$$q_s' \approx \frac{\partial^2 q_s}{\partial T^2} T'^2. \tag{112}$$

Substituting (91) into (103) and using (112), (104) and (105) we obtain

$$p_q'(\mathbf{x}, t) = -\frac{\rho_0 \gamma L_\nu}{4\pi c_s^2 |\mathbf{x}|} \frac{\partial^2 q_s}{\partial T^2} \frac{\partial^2}{\partial t^2} \int T'(\mathbf{x}', t) T'(\mathbf{x}', t) d^3\mathbf{x}', \tag{113}$$

which corresponds to a monopole radiation field.

For total acoustic power radiated by a monopole source related to moisture we have

$$N_q = \frac{4\pi |\mathbf{x}|^2}{\rho_0 c_s} \langle p'(\mathbf{x}, t) p'(\mathbf{x}, t) \rangle \sim \frac{\rho_0 \gamma^2 L_\nu^2}{c_s^5} \left(\frac{\partial^2 q_s}{\partial T^2} \right)^2$$
$$\times \frac{\partial^4}{\partial t^4} \int d^3\mathbf{x}' d^3\mathbf{x}'' \langle T'(\mathbf{x}', t) T'(\mathbf{x}', t) T'(\mathbf{x}'', t) T'(\mathbf{x}'', t) \rangle \tag{114}$$

Fluctuations of temperature in different regions of the turbulent flow separated by distances greater then length scale l of energy containing eddies are not correlated and therefore the integral in Eq.(114) can be estimated as $F_1 l^3 \Delta T^4$, where F_1 is the volume occupied by saturated moist air turbulence. Also taking into account that the characteristic timescale of the process is the turn over time of energy containing turbulent eddies l/v we finally obtain

$$N_q \sim \frac{\rho_0 \gamma^2 L_\nu^2 \Delta q^2 M_t^4}{l c_s} F_1 = \frac{\gamma^2 L_\nu^2 \Delta q^2}{M_t^4 c_s^4} \frac{F_1}{F} N_L, \tag{115}$$

where Δq is the rms of humidity mixing ratio perturbations. For the acoustic power of the source related to gas mass production we obtain

$$N_m \sim \frac{\rho_0 a^2 c_s^3 \Delta q^2 M_t^4}{l} F_1 = \frac{a^2 \Delta q^2}{M_t^4} \frac{F_1}{F} N_L. \tag{116}$$

2.3 Application to infrasound generation by supercell convective storms

In this section we apply our findings to study infrasound generation by tornadic convective storms. Taking typical parameters of supercell storms to be $v \sim 5$ ms^{-1}, $\Delta T \sim 3°$ K (Gossard and Hooke 1975; Bluestein 1992), $T = 270°$ K and $c_s = 330$ m/s and using Eqs. (108) and (109) we see that the dipole radiation related to temperature inhomogeneities is of the same order as the radiation of Lighthill's quadrupole source (Akhalkatsi et $al.$ 2004).

Combining Eqs.(115)-(116) and using $L_\nu \approx 2.5 \times 10^6$ m^{2}s^{-2} and $\gamma \approx 1.4$ we obtain

$$\frac{N_q}{N_m} \approx \left(\frac{\gamma L_\nu}{c_s^2} \right)^2 \approx 10^3, \tag{117}$$

Therefore the acoustic power of the source related to gas mass production is negligible compared to the radiation related to heat production.

Estimation of Δq is a bit more difficult. For saturation specific humidity we use Bolton's formula (Bolton 1980)

$$q_s \approx \frac{3.8}{p_0} \exp \left(\frac{17.67 T_c}{T_c + 243.5} \right), \tag{118}$$

where $T_c = T - 273.15$ is the temperature in degree Celsius and p_0 is atmospheric pressure in mb. Taking Eq. (112) into account and using $p_0 \approx 800$ mb, we obtain

$$\Delta q \approx \frac{6.8 \cdot 10^4}{(243.5 + T_c)^4} \exp\left(\frac{17.67 T_c}{T_c + 243.5}\right) \Delta T^2 \equiv f(T_c)\frac{\Delta T^2}{T^2}. \qquad (119)$$

Note that due to the numerator in the exponent, $f(T_c)$ strongly depends on temperature, e.g., $f(T_C = 10°)/f(T_C = 0°) \approx 2$.

Using Eqs. (108) and (115) we obtain

$$\frac{N_q}{N_L} \approx \left[\frac{\gamma L_\nu}{c_s^2}\right]^2 \left[\frac{\Delta T}{M_t T}\right]^4 \left[\frac{F_1}{F}\right]^2 f^2(T_c). \qquad (120)$$

For our analysis we have assumed that $T_c = 0°$C, ($f(0) \approx 1.66$) and $F \approx 125$ km^3 (Georges and Greene 1975) and for the estimation of F_1 we note that the saturation level of atmospheric convection is usually at the height $\approx 1 - 1.5$ km. Also taking into account that $f(T_c)$ rapidly drops with the decrease of T_c, one can expect that the main acoustic radiation will be produced at the heights $(1.5 - 4)$ km and consequently we assume $F_1 \approx 0.5F$, then Eq. (120) yields

$$\frac{N_q}{N_L} \approx 2 \times 10^2. \qquad (121)$$

Therefore, we conclude that infrasound radiation of a supercell storm should be dominated by monopole sources related to heat production during water condensation. Also assuming that the constant of proportionality in Eq. (108) is equal to 100 (Goldstein 1976; Georges and Greene 1975) and $l \approx 10$ m, then the total radiation power is

$$N_q \approx 2.4 \times 10^7 \text{ watts}, \qquad (122)$$

in qualitative agreement with observations (Bowman and Bedard 1971; Bedard and Georges 2000; Georges and Greene 1975; Georges 1973).

As was mentioned previously, the characteristic frequency of the emitted acoustic waves is $\Omega \sim v/l$, and using characteristic values of the velocity and length scale we obtain $\tau \sim 10$ s for the period.

2.4 Discussion and Summary

In this section we have considered acoustic radiation from turbulent convection in the framework of a generalized acoustic analogy, taking into account effects of stratification, temperature fluctuations and moisture in the air. We have simplified the analysis assuming low Mach number turbulence. In addition we have considered acoustic waves with wavelengths much shorter than the stratification lengthscale and dropped nonlinear effects of acoustic wave propagation. Analysis shows the existence of monopole sources related to heat and mass production during the condensation of moisture in the saturated moist air turbulence. This is in addition to the Lighthill's quadrupole and known dipole sources of sound related to stratification and temperature fluctuations. It has been shown that for typical parameters of the strong convective storms infrasound radiation should be dominated by monopole sources related to the moisture of the air. The total power of the source related to moisture is of order 10^7 watts, in qualitative agreement with observations of strong convective storms (Bowman and Bedard 1971; Bedard and Georges 2000; Georges and Greene 1975).

3   Spectrum of infrasound radiation from supercell storms

This section represents an extension of the study performed in the section 2. Namely, we extended earlier study in two directions. Firstly, we perform detailed spectral analysis of a monopole source related to heat production during the condensation of moisture. Assuming homogeneous and stationary turbulence we calculate the spectrum of acoustic radiation. Secondly, we perform detailed analysis of the sound generated by a monopole source as well as infrasound observations and present a qualitative explanation of the observed high correlation between intensity of low frequency infrasound signals from supercell storms and the probability of later tornado formation.

We show that acoustic power of a monopole source related to the moisture of the air strongly depends on the same parameters that are the most promising in discriminating between nontornadic and tornadic supercells according to the recent study of tornadogenesis (Markowsky and Richardson 2008).

In particular, low lifting condensation level (LCL) is known to favor significant tornadoes (Rasmussen and Blanchard 1998; Thompson *et al.* 2003). On the other hand, low LCL height means that air in the updraft is saturated at lower heights and consequently has a higher temperature at the level of saturation. We show that the increase of temperature causes rapid enhancement of monopole acoustic power related to heat production during condensation of moisture.

Another widely used supercell and tornado forecasting parameter is supercell environmental convective available potential energy (CAPE). It is known that high values of CAPE (especially, occurring closer to the surface) assist tornado formation (Weisman and Klemp 1982; Rotunno and Klemp 1982; Rasmussen 2003; Rasmussen and Blanchard 1998; Thompson *et al.* 2003). Furthermore, high values of CAPE means high updraft velocity and therefore the increased rms of turbulent velocities, which results in a strong enhancement of total

acoustic power.

The section is organized as follows: General formalism is presented in subsection 3.1. Spectral analysis of acoustic radiation is performed in subsection 3.2. Correlation between intensity of infrasound radiation by supercell storm and probability of tornado formation is discussed in section 3.3. Conclusions are given in section 3.4.

3.1 General formalism

As was discussed in the previous section the dynamics of moist turbulent atmosphere is governed by the continuity, Euler, heat, humidity and ideal gas state equations:

$$\frac{D\rho}{Dt} + \rho \nabla \cdot \mathbf{v} = 0, \tag{123}$$

$$\rho \frac{D\mathbf{v}}{Dt} = -\nabla p - \rho \nabla \Phi, \tag{124}$$

$$T\frac{Ds}{Dt} = -L_\nu \frac{Dq}{Dt}, \tag{125}$$

$$\rho = \frac{p}{RT}\frac{1}{1 - q + q/\epsilon} = \frac{p}{RT}\frac{1}{1 + aq}, \tag{126}$$

where $\mathbf{v}$, ρ and p are velocity, density and pressure, respectively; $D/Dt \equiv \partial/\partial t + \mathbf{v} \cdot \nabla$ is Lagrangian time derivative; L_ν is the latent heat of condensation and q is the humidity mixing ratio

$$q \equiv \frac{\rho_\nu}{\rho}. \tag{127}$$

Here ρ_ν is the mass of water vapor in a unit volume; Φ is gravitational potential energy per unit mass and $\nabla \Phi \equiv -\mathbf{g}$. $\epsilon \equiv m_\nu/m_d \approx 0.622$ is the ratio

of molecular masses of water and air; $a = 0.608$ and R is the universal gas constant.

In the set of Eqs. (123)-(126) diffusion and viscosity effects are neglected due to the fact that they have a negligible influence on low frequency acoustic wave generation and propagation.

In the subsection 2.1. the equation governing sound generation by turbulence was obtained using the standard procedure of Lighthill's acoustic analogy (Goldstein 2002):

$$\frac{1}{\rho_0}\left(\frac{1}{c_s^2}\frac{\partial^2}{\partial t^2} - \nabla^2\right)p' = S_L + S_T + S_\gamma + S_q + S_m \tag{128}$$

with

$$S_L \approx \nabla \cdot (\omega \times \mathbf{v}), \tag{129}$$

$$S_T \approx -\nabla \cdot (T\nabla s), \tag{130}$$

$$S_\gamma = p\frac{\partial \gamma}{\partial q}\left(\frac{\partial q}{\partial t}(\mathbf{v}\nabla)p - \frac{\partial p}{\partial t}(\mathbf{v}\nabla)q\right), \tag{131}$$

$$S_m \approx \frac{a}{1+aq}\frac{\partial^2 q}{\partial t^2}, \tag{132}$$

$$S_q \approx -\frac{\gamma L_\nu}{c_s^2}\frac{\partial^2 q}{\partial t^2}. \tag{133}$$

We have simplified the analysis assuming low Mach number turbulence. In addition we have considered acoustic waves with wavelengths much shorter than the stratification lengthscale and dropped nonlinear effects of acoustic wave propagation.

First three terms on the right hand side of Eq. (128) represent well known sources of sound: the first term represents Lighthill's quadrupole source (Lighthill

1952); the second term is a dipole source related to temperature fluctuations (Goldstein 1976); S_γ is a monopole source related to variability of adiabatic index and usually has negligible acoustic output (Howe 2001). As it was shown in Akhalkatsi and Gogoberidze (2009), in the case of saturated moist air turbulence there exists two additional monopole sources of sound, S_q and S_m, related to nonstationary heat and mass production during condensation of moisture, respectively.

As it was shown in the subsection 2.2. turbulent mixing of saturated air with different temperatures leads to two effects important for sound generation: production of heat and decrease of gas mass.

As it was also shown in the subsection 2.3., for typical parameters of supercell storms acoustic radiation is dominated by a monopole source related to the heat production S_q.

The total acoustic power can be estimated as

$$N_q \sim \frac{\rho_0 \gamma^2 L_\nu^2 \Delta q^2 M_t^4}{l c_s} F_1, \tag{134}$$

where Δq is the rms of humidity mixing ratio perturbations; l is the length scale of energy containing turbulent eddies; $M_t \equiv v/c_s \ll 1$ is turbulent Mach number and F_1 is the volume occupied by saturated moist air turbulence.

For typical parameters S_q is much greater, than other sources of sound and two orders of magnitude stronger then Lighthill's quadrupole source.

3.2 Spectral Decomposition

In this section we study the spectrum of acoustic radiation related to S_q. Dropping all other source terms (128) reduces to the inhomogeneous wave equation

$$\frac{1}{\rho_0} \left(\frac{1}{c_s^2} \frac{\partial^2}{\partial t^2} - \nabla^2 \right) p' = S_q. \tag{135}$$

Using standard methods for spectral analysis of the inhomogeneous wave equation (Goldstein 1976; Howe 2001; Gogoberidze *et al.* 2007), after a long but straightforward calculation, for the spectrum of temperature fluctuations $I(\mathbf{x}, \omega)$ we obtain

$$I(\mathbf{x}, \omega) = \frac{\omega^4 \pi \rho_0 \gamma^2 L_\nu^2}{2c_s^5 |\mathbf{x}|^2} \left(\frac{\partial^2 q_s}{\partial T^2} \right)^2 \int \mathrm{d}^3 \mathbf{x}' H \left(\mathbf{x}', \frac{\mathbf{x}}{|\mathbf{x}|} \omega, \omega \right), \qquad (136)$$

where $H(\mathbf{x}', \mathbf{k}, \omega)$ is a spectral tensor of temperature fluctuations and represents a Fourier transform of a two point time delayed forth order correlation function of temperature fluctuation.

Equation (136) allows to calculate the spectrum of sound radiated by a monopole source related to the moisture, if statistical properties of the turbulent source can be determined. For our calculations we consider the Von Karman model of stationary and homogeneous turbulence, which is given by (Hinze 1975)

$$E_k = C_K \varepsilon^{2/3} k_0^{-5/3} \frac{(k/k_0)^4}{[1 + (k/k_0)^2]^{17/6}}. \qquad (137)$$

for $k < k_d$ and $E_k = 0$ for $k > k_d$, where $2\pi/k_d$ is the dissipation length scale.

The Von Karman spectrum reduces to the Kolmogorov spectrum in the inertial interval ($k \geq k_0$), but also satisfactorily describes the energy spectrum in the energy containing interval, which is a dominant contributor to acoustic radiation.

As is known (Monin and Yaglom 1975), temperature fluctuations of homogeneous isotropic and stationary turbulence behaves like a passive scalar and therefore has the same spectrum as velocity fluctuation. Therefore for the spectral function of temperature fluctuation $F(\mathbf{k}, \tau)$, which is spatial Fourier transform of temperature correlation function $\Theta(\mathbf{r}, \mathbf{t}) = \langle \mathbf{T}'(\mathbf{x} + \mathbf{r}, \mathbf{t}) \mathbf{T}'(\mathbf{x}, \mathbf{t}) \rangle$, we assume

$$F(\mathbf{k}, \tau) = \frac{Q_k}{4\pi k^2} f(\eta_k, \tau), \tag{138}$$

where

$$Q_k = \Delta T^2 k_0^{-1} \frac{(k/k_0)^4}{[1 + (k/k_0)^2]^{17/6}}. \tag{139}$$

In equation Eq. (138) $\triangle T$ is rms of the temperature fluctuation, η_k is the autocorrelation function defined as

$$\eta_k = \sqrt{\frac{k^3 E_k}{2\pi}} \tag{140}$$

and $f(\eta_k, \tau)$ characterizes the temporal decorrelation of turbulent fluctuations, such that it becomes negligibly small for $\tau \gg 1/\eta_k$.

For $f(\eta_k, \tau)$ we use a square exponential time dependence (Kraichnan 1964)

$$f(\eta_k, \tau) = \exp\left(-\frac{\pi}{4} \eta_k^2 \tau^2\right). \tag{141}$$

For a homogeneous turbulence two point time delayed forth order correlation function of temperature fluctuations $R(\mathbf{x}', \mathbf{x}' + \mathbf{r}, \tau)$ is related to the temperature correlation function by means of the following relation (Monin and Yaglom 1975)

$$R(\mathbf{x}', \mathbf{x}' + \mathbf{r}, \tau) = 2 \langle T'(\mathbf{r}, \tau) T'(\mathbf{r}, \tau) \rangle \langle T'(\mathbf{r}, \tau) T'(\mathbf{r}, \tau) \rangle. \tag{142}$$

Using Eqs. (138),(140),(141) and the convolution theorem we find

$$H(\mathbf{k}, \omega) = 2 \int d\mathbf{k}_1^3 d\omega_1 g(\mathbf{k}_1, \omega_1) g(\mathbf{k} - \mathbf{k}_1, \omega - \omega_1), \tag{143}$$

where

$$g(\mathbf{k}, \omega) = \frac{Q_k}{4\pi^2 \eta_k} \exp\left(-\frac{\omega^2}{\pi \eta_k^2 k^2}\right). \tag{144}$$

For low Much number turbulence one can use the so called aeroacoustic approximation (Goldstein 1976), which for the Fourier spectrum implies that in Eq. (136) instead of $H(\mathbf{x}', \omega\mathbf{x}/|\mathbf{x}|, \omega)$ one can set $H(\mathbf{x}', 0, \omega)$.

Performing the integration with respect to frequency in Eq. (143) as well as angular variables in wave number space we obtain

$$H(0,\omega) = \frac{\sqrt{2}}{4\pi^2} \int_{k_0}^{k_d} \mathrm{d}k \frac{Q_k^2}{k^2 \eta_k} \exp\left(-\frac{\omega^2}{2\pi\eta_k^2}\right). \tag{145}$$

The aeroacoustic approximation simplifies finding asymptotic limits for the spectrum. In the low-frequency regime, taking the limit $\omega \to 0$ we obtain

$$H(0,\omega) \sim \frac{1}{10\pi^{3/2}} \frac{\Delta T^4}{k_0^4 M c_s}. \tag{146}$$

For the spectrum this means $I(\mathbf{x}, \omega) \sim \omega^4$. Physically, these frequencies are lower than the lowest characteristic frequency in the problem, corresponding to the eddy turnover time on the energy containing scale.

At high frequencies $\omega \gg k_0 M R^{1/2}$, the integral in Eq. (145) is dominated by the contribution from its upper limit and we get

$$H(0,\omega) \sim \frac{3}{8\pi^{3/2}} \frac{\Delta T^4}{k_0^2} \frac{M c_s}{\omega^2} \exp\left(-\frac{\omega^2}{k_0^2 M^2 c_s^2 R}\right) \tag{147}$$

and

$$I(\mathbf{x}, \omega) \sim \omega^2 \exp\left(-\frac{\omega^2}{k_0^2 M^2 c_s^2 R}\right). \tag{148}$$

The functional form of the high-frequency suppression is determined by the specific form of the time autocorrelation function of turbulence Eq. (141) (Kraichnan 1964), but for any autocorrelation the amplitude of emitted waves should be very small in this band. Physically, this limit corresponds to radiation frequencies which are larger than any frequencies of turbulent motions; consequently, no scale of turbulent fluctuations generates these radiation frequencies directly, and the resulting small radiation amplitude is due to the sum

of small contributions from many lower-frequency source modes. Since the integral is dominated by the upper integration limit, the highest-frequency source fluctuations (which contain very little of the total turbulent energy) contribute most to this high-frequency radiation tail.

In the intermediate frequency regime, $k_0 M c_s < \omega < k_0 M c_s R^{1/2}$, the integral in Eq. (145) is dominated by the contribution around k_1, where $\eta_{k_1} \approx \omega$. The width of the dominant interval is $\Delta k_1 \sim k_1$. Physically, this implies that radiation emission at some frequency in this range is dominated by turbulent vortices of the same frequency. Consequently, for the inertial interval we obtain following estimate

$$H(0, \omega) \simeq \frac{1}{3\pi^{3/2}} \frac{\Delta T^4}{k_0^4 M c_s} \left(\frac{k_0 M c_s}{\omega} \right)^{15/2} \tag{149}$$

and

$$I(\mathbf{x}, \omega) \sim \omega^{-7/2}. \tag{150}$$

We performed numerical integration of Eq. (145) for the Von Karman model of turbulence and determined normalized spectrum of acoustic radiation to be

$$I_N(\nu) = \frac{4\sqrt{2}\pi c_s^2 |\mathbf{x}|^2}{\rho_0 \gamma^2 L_\nu^2 k_0 v_0^4 \Delta T^4 F_1} I(\mathbf{x}, \omega). \tag{151}$$

The normalized spectrum for characteristic length scale of energy containing eddies $l = 2\pi/k_0 = 15$ m and characteristic rms velocity $v_0 = 5$ m s^{-1} is presented in Fig. 11. As can be seen for these typical parameters the peak frequency of infrasound radiation is $\nu_{peak} \approx 0.8$ Hz.

As shown in the subsection 2.3. the peak frequency of acoustic radiation is inversely proportional to the turnover time of energy containing turbulent eddies $\nu_{peak} \sim v_0/l$, whereas total acoustic power is proportional to v_0^4, ΔT^4 and inversely proportional to l.
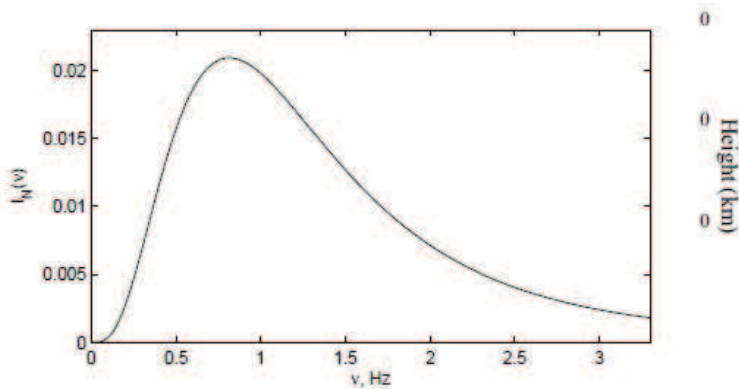
Figure 11: Normalized spectrum of acoustic radiation for Von Karman turbulence.

3.3 Infrasound correlation with tornadoes

Severe storm forecasting operations are based on several large scale environmental, storm scale, meso-beta scale kinematic and thermodynamic parameters (Davies-Jones 1993; Lemon and Doswell 1979; Markowski *et al.* 1998, Markowski *et al.* 2002), used to study the potential of severe weather, thunderstorm structure and organization to produce tornadoes.

Recent climatological studies of thunderstorms using real-time radar data combined with observations of near-storm environment have been focused on the utility of various supercell and tornado forecast parameters (CAPE, Storm Relative Helicity - SRH, Bulk Richardson number - BRN and other parameters).

Two parameters have been established to be the most promising in discriminating between nontornadic and tornadic supercells: boundary layer water vapor concentration (LCL hight) and low level vertical wind shear (Markowski and Richardson 2008; Rasmussen 2003; Thompson and Edwards 2000).

Examining a baseline climatology of parameters commonly used in supercell thunderstorm forecasting and research, Rasmussen and Blanchard (1998) established that the parameter that shows the most utility for discriminating between soundings of supercells with significant tornadoes and supercells with-

out significant tornadoes is LCL height. The height of the LCL appeared to be generally lower for supercells with significant tornadoes than those without. Rasmussen and Blanchard (1998) also found that for storms producing large (at least 5-cm wide) hail only, without at least F2 strength tornadoes, the LCL heights were significantly higher than for ordinary thunderstorms. In their study half of the tornadic supercells soundings had LCLs below 800 m, while LCL heights above about 1200 m were associated with decreasing likelihood of significant tornadoes. They concluded that stronger evaporational cooling of moist downdraft leads to greater outflow dominance of storms in high LCL settings and low heights increase the likelihood of supercells being tornadic.

The work of Thompson and Edwards (2000) on assessing utility of various supercell and tornado forecasting parameters supports the finding that supercells above deeply mixed convective boundary layers, with relatively large dew point depressions and high LCL, often do not produce tornadoes even in environments of large CAPE and/or vertical shear. They found the LCL to be markedly lower for supercells producing significant tornadoes than for those producing weak tornadoes, which were in turn lower than for nontornadic supercells. Particularly, no strong and violent tornadoes occurred for supercells with LCL > 1500 m.

Studying the relationship between Rear flank downdraft (RFD) thermodynamic characteristics and tornado likelihood Markowski *et al.* (2002) found that low LCL favors formation of significant tornadoes because the boundary layer relative humidity somehow alters the RFD and outflow character of supercells. Relatively warm and buoyant RFDs, which are supposed to be necessary for the genesis of significant tornadoes, were more likely in moist low-level environments than in dry low-level environments (Markowski *et al.* 2002). It appeared that relatively dry boundary layers, characterized by higher LCLs, support more low-level cooling through the evaporation of rain, leading to stronger outflow, which could have been decreasing the likelihood of signif-

icant tornadoes in supercells. These are possible explanations for finding that the LCL height is generally lower in soundings associated with tornadic supercells versus nontornadic (Rasmussen and Blanchard 1998; Thompson and Edwards 2000).

Thompson *et al.* (2003) reinforced the findings of previous studies related to LCL height as an important discriminator between significantly tornadic and nontornadic supercells and concluded that the differences in LCL heights across all storm groups studied were statistically significant, though the differences appeared to be operationally useful only when comparing significantly tornadic and nontornadic supercells. The lower LCL heights of the significantly tornadic storms supported the hypothesis of Markowski *et al.* (2002) that increased low-level relative humidity (RH) may contribute to increased buoyancy in the rear flank downdraft and an increased probability of tornadoes.

In idealized numerical simulations Markowski *et al.* (2003) investigated the effects of ambient LCL and the precipitation character of a rain curtain on the thermodynamic properties of downdraft, and ultimately on tornado intensity and longevity. The simulations were consistent with the observation that high boundary layer relative humidity values (i.e., low LCL height and small surface dewpoint depression) are associated with relatively warmer RFDs and more significant tornadogenesis than environments of relatively low boundary layer relative humidity. These findings of low LCL favoring significant tornadoes could explain observed high correlation between low frequency infrasound signals from supercell storm and later tornado formation.

Acoustic power of a monopole source related to the heat production during condensation of moisture can been estimated as (Akhalkatsi and Gogoberidze 2009):

$$N_q \sim \frac{\rho_0}{l c_s} [\gamma L_\nu]^2 \Big[\frac{M_t \Delta T}{T} \Big]^4 f^2(T_c) F_1, \tag{152}$$

where

$$f(T_c) \approx 6.8 \cdot 10^4 \frac{273.15 + T_c}{(243.5 + T_c)^4} \exp\left(\frac{17.67 T_c}{T_c + 243.5}\right). \tag{153}$$

and $T_c = T - 273.15$ is the temperature in degree Celsius.

Due to the numerator in the exponent, $f(T_c)$ strongly depends on temperature, e.g., $f(T_C = 10°)/f(T_C = 0°) \approx 2$ and according to multiplier $f^2(T_c)$ in Eq. (152), increase of saturated air temperature causes rapid enhancement of total acoustic power radiated by a monopole source.

On the other hand, low LCL height means low level air in the updraft motion being saturated and consequently, higher temperature of saturated moist air. Therefore, the lower LCL heights contribute to increased total acoustic power radiated by a monopole source related to the heat production during the condensation of moisture. As a result, enhanced low frequency infrasound signals from supercell storm appear to be in strong correlation with an increased probability of tornadoes.

It is also known (Weisman and Klemp 1982; Rotunno and Klemp 1982; Rasmussen 2003; Rasmussen and Blanchard 1998; Thompson *et al.* 2003)that high values of supercell CAPE assist tornado formation. Indeed, high values of CAPE lead to an increase of the updraft persistence and thunderstorm activity and therefore increase probability of tornado formation.

According to recent studies relatively larger CAPE occurs closer to the surface, which could produce more intense low-level stretching of vertical vorticity required for low-level mesocyclone intensification and perhaps tornadogenesis (Rasmussen 2003, McCaul 1991; McCaul and Weisman 1996) is associated with low LCLs. Rasmussen (2003) found the 03-km above ground level (AGL) CAPE to be possibly important in discriminating between environments supportive of significant tornadoes and those that are not.

High values of CAPE mean high updraft velocity caused by large low-level accelerations and increased rms of turbulent velocities. According to Eq. (152) $N_q \sim M_t^4$, Therefore increasing rms of turbulent velocities results in strong

enhancement of total acoustic power.

3.4 Conclusions

In this section we have performed detailed spectral analysis of a monopole source of sound related to heat production during condensation of moisture, which is supposed to be dominant in the infrasound radiation observed from strong convective storms. We have also discussed the relationship between the acoustic power of this source and certain significant tornado forecast parameters. Particularly, low LCL, which is known to favor significant tornadoes (Rasmussen and Blanchard 1998; Thompson *et al.* 2003) implying warmer air at the level of saturation. We have shown that the increase of temperature causes rapid enhancement of acoustic power. High values of CAPE (especially, occurring closer to the surface), which assist tornado formation (Weisman and Klemp 1982; Rotunno and Klemp 1982; Rasmussen 2003; Rasmussen and Blanchard 1998; Thompson *et al.* 2003), mean high updraft velocity and therefore, increased rms of turbulent velocities, which results in strong enhancement of total acoustic power.

ISNeT data combined with the information from Doppler Radar may help to improve tornado forecast and reduce false alarms from non-tornadic supercells. Recent studies comparing ISNeT output with occurrences of tornadoes (Bedard *et al.* 2004a) and correlating ISNeT signals with detailed radar output (Szoke *et al.* 2004) show, that infrasound of a tornadic thunderstorm is much stronger than the infrasound of a nonsevere weather system. Correlation between the intensity of infrasound signals and probability of later tornado formation indicates the potential for discriminating between supercells that produce tornadoes and those that do not. Therefore, information from an infrasound detecting system may help to determine potentially tornadic storms.

4 Wave generation by turbulence in the solar chromosphere

The mechanism of upper chromospheric heating in the Sun has been an important topic of research for many years since chromospheric heating produces UV emissions that can only occur in an enhanced electron temperature medium. The observations of line and continuum emissions by non-active solar surface indicated that chromospheric temperatures are around 6000-7000 K, much higher than those that can be expected for a plasma in radiative equilibrium.

In the quiet Sun the radiative losses are an order of magnitude larger than those in the much hotter corona. Interpretation of the observations made during empirical modeling of the chromospheric structure, that was carried out using Skylab UV (ultra violet) observations (e.g. Vernazza *et al.* 1981, Fontenla *et al.* 1991 1993), required an understanding of the chromospheric heating physical mechanism.

Figure 12 (Fontenla *et al.* 2008) shows the ratio of radiative losses to total hydrogen density for several spectral bands and the total for wavelengths between 300 nm and 3 micron. This figure indicates the near radiative equilibrium character of the low chromosphere and that radiative losses are important only in the photosphere and in the upper chromosphere. The upper chromospheric radiative losses per H atom for wavelengths shorter than 400 nm are larger than in the photosphere.

Convective zone of the Sun carries enough energy via convective motions to account for energy dissipation in the chromosphere. Carlsson and Stain (1992) carried out theoretical and very detailed numerical studies of the idea proposed by Biermann (1946) and Schwarzschild (1948), that the quiet-Sun chromospheric regions are heated by transient acoustic waves generated in the convective zone. However, measurements of the acoustic energy flux are not consistent with the amount of the energy needed for the heating of the whole chromosphere (Fossum and Carlsson 2005).
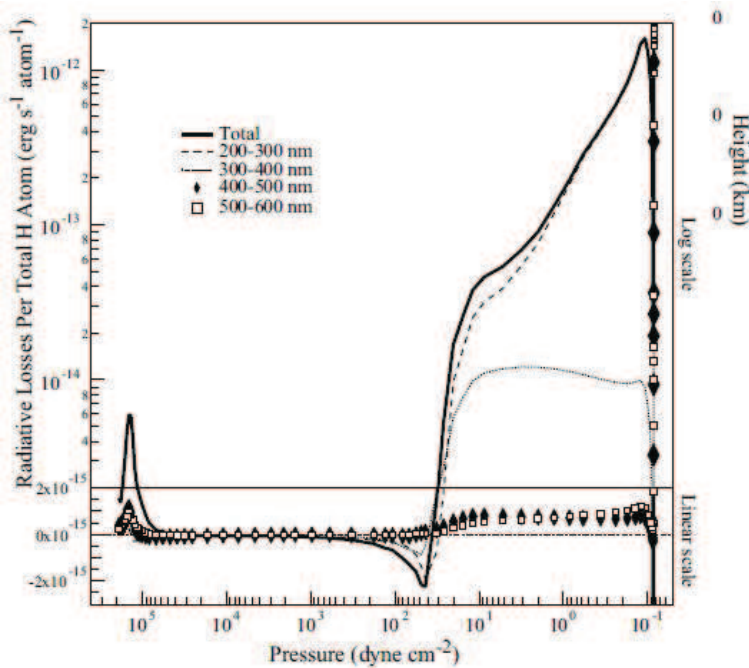
Figure 12: Ration of radiative losses to hydrogen density computed for chromospheric model SRPM 306.

Observed correlation between the UV intensity distribution with magnetic fields of the quiet-Sun indicate a relationship between chromospheric heating and magnetic fields.

As a possible scenario for explaining of chromospheric heating, the impulsive nano-flares related to magnetic reconnection events, were proposes as a source of UV emission (Parker 1988; Sturrock 1999). Although, observed numerous transient brightening in the Sun are not sufficiently frequent and energetic to account for the persistent UV emission and chromospheric heating (Aschwanden *et al.* 2000, Carlsson 2007). In principle ion-cyclotron resonance (see e.g. Akhalkatsi and Machabeli 2000) can also affect chromospheric heating process.

As it has been shown recently, the magnetoacoustic waves generated locally, inside or in the vicinity of the magnetic flux tubes (Hasan and van Ballegooijen 2008) can be responsible for heating the quiet-Sun chromosphere. Erdelyi and James (2004) suggested that random Alfven waves can initiate ion-neutral collisions and the consequent heating of the upper chromosphere. This mechanism also can explain the formation of spicules.

An alternative mechanism for chromospheric heating is the resistive dissipation of electric currents (Rabin and Moore 1984; Goodman 2004). However, recent studies (Socas-Navarro 2007) has shown, that resistive current dissipation contributes to heating the sunspot chromosphere, but it is not the dominant factor. The reason is that large electrical conductivity of solar plasma requires strong variations of the magnetic field and extremely localize electric currents to produce enough energy dissipation, as was suggested from the analysis of the spectropolarimetric observational data of a sunspot from photospheric to chromospheric level.

Recent studies (Liperovsky *et al.* 2000; Fontenla 2005; Fontenla *et al.* 2008) considered plasma effects in the low chromosphere and suggested that the Farley-Buneman (Farley 1963; Buneman 1963) plasma instability, driven by convective motions of neutral atoms, can be responsible for dissipating the energy into chromospheric heating in the Sun and other cool stars of solar type that have a partially ionized chromosphere. They proposed a mechanism for chromospheric heating due to the rapid onset of the Farley-Buneman instability marking the start of the upper chromosphere and strong magnetic heating.

In the E layer of the Earth ionosphere the Earth's electric and magnetic field produces currents and drive the Farley-Buneman instability that creates plasma irregularities at heights where the electrons are strongly magnetized.

Similar mechanism can be responsible for chromospheric heating. Fontenla *et al.* (2008) concluded that Farley-Buneman instability can be triggered by the cross-field motions of the neutral component of the partially ionized gas at velocities in excess of the ion acoustic velocity, which they acquire through collisions with the much denser chromospheric neutral atoms. This instability should be present at least in the upper half of the chromosphere because electrons become strongly magnetized just above the photosphere, while heavy ions and protons become magnetized only at the top of the chromosphere. Earlier, the analysis of Liperovsky *et al.* (2000) had indicated that the Farley-Buneman

instability might operate in the chromosphere at heights $h > 1000$ km.

However, in recent study of Farley-Buneman instability in the solar chromosphere Gogoberidze *et al.* (2009) showed that even though the Farley-Buneman instability can sporadically appear in the chromosphere, it cannot be responsible for quasi-steady chromospheric heating. They concluded that the Farley-Buneman instability at small lencth scales cannot be excluded, but the heating produced by the Farley-Buneman instability cannot compete with the frictional heating under chromospheric conditions. In the presence of strong cross-field currents it can produce small-scale, 0.1-3 m, density irregularities in the solar chromosphere. These irregularities can cause scintillations of radio waves with similar wavelengths and provide a tool for remote diagnostics of strong cross-field currents in the solar chromosphere.

4.1 Semiempirical models of the solar atmosphere

Two complementary approaches, semiempirical and theoretical, are used for understanding the solar and stellar atmospheres. Reconciling these techniques to explain spatial and temporal structure in both high- and low-resolution observations provides a minimal set of empirically derived parameters that determine the atmosphere. Both approaches are important for understanding physical processes in the Sun and stars via spectroscopy since our knowledge of some of the physical processes is not fully understood, for example, chromospheric magnetic-heating mechanism.

In purely theoretical modeling of physical processes the distribution of temperature and density are computed from first principles and from initial and boundary conditions, e.g., numerical simulations of magneto-convection. Numerical simulations based on energy balance provide a physical description of the photosphere and deeper layers but underlying approximations, assumptions, and the details of the calculations need to be fully investigated to quan-
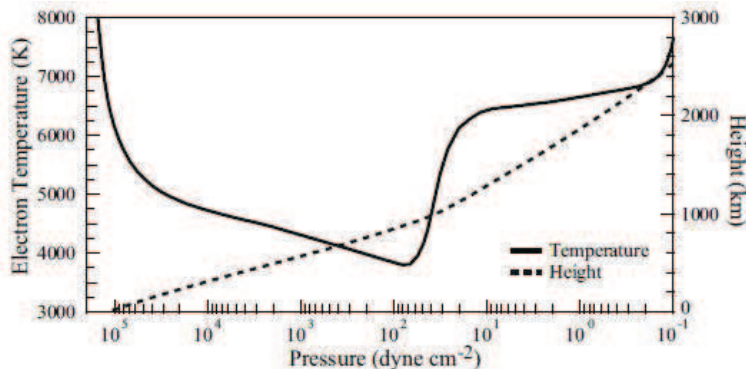
Figure 13: Temperature and height structure of the chromospheric model SRPM 306.

titatively match observations that span a wide wavelength range.

Semiempirical atmospheric modeling contrast with, but does not oppose, the purely theoretical approach. These models characterize the temperature and density variations as a function of height above an arbitrary solar radius and the distribution of other physical parameters, which are derived by comparing the observed spectrum with calculations performed on trial models based on solving equations that describe the structure and the detailed transport of radiation through the model atmosphere.

The early models of the quiet-Sun atmosphere (Gingerich and Jager 1968; Gingerich *et al.* 1971) were advanced by Vernazza *et al.* (1981). Fontenla *et al.* (1999) developed a set of semiempirical models for the quiet and active Sun. Subsequently, several modifications of these models were made (Fontenla *et al.* 2005; Fontenla *et al.* 2007) to account for main quiet- and active Sun component features as observed at moderate spatial and temporal resolution.

These semiempirical models of the solar photosphere are derived from the observed visible, infrared (IR) and UV continuum and from photospheric line radiation.

Figure 13 shows the temperature, height, and pressure profiles from one-dimensional model of the solar atmosphere (called SRPM 306) of the quiet-Sun chromosphere.
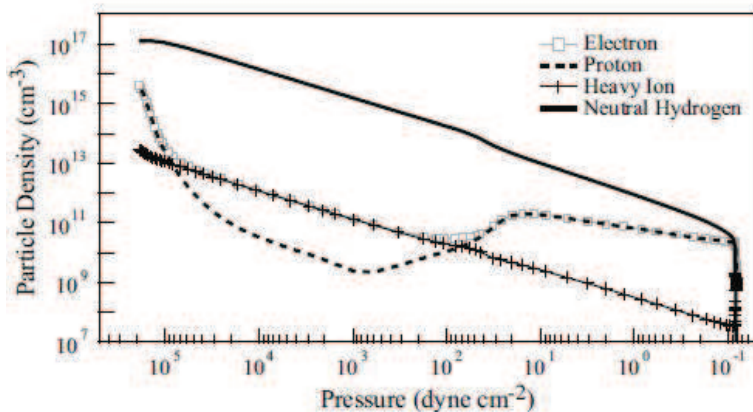
Figure 14: Particle densities in the chromospheric model SRPM 306.

4.2 Wave generation by turbulence in partially ionized plasma of solar chromosphere

Solar atmosphere is significantly superadiabatic and possess ionization zones. The chromospheric gas is essentially composed by neutral H and He. In the lower chromosphere and near the temperature minimum the proton contribution to the charge balance is small and the positive charge is supplied by the singly ionized heavy metals. The elements with low first-ionization-potential (e.g., Si, Mg, Fe, Ca, etc.) are predominately singly ionized in the lower- and upper-chromospheric layers because of the temperature and density values. The ionization degree depends on the temperature, thus when temperature steeply rises to the chromospheric plateau (see Fig. 13) protons are the main positive charge in the upper chromosphere and although their density is still much smaller than the neutral H particle density, the ionization degree is quite high $(10^{-2} - 10^{-4})$. Figure 14 (Fontenla et $al.$ 2008) shows the electron, proton, and ion densities in the model SRPM 306.

The novel mechanism of acoustic wave generation by turbulence related to the non-stationary heat sources is applied to the study of physical processes in the solar chromosphere (Akhalkatsi and Gogoberidze 2011). As it was mentioned above, temperature is not uniform in the chromosphere (see Fig. 13).

91

Velocity fluctuations invoke mixing of partially ionized plasma from different regions of the chromosphere. This causes temperature fluctuations, which on their turn initiate fluctuations of the ionization level. The later automatically implies (like saturated moist air in the Earth's atmosphere) presence of the non-stationary heat fluctuations in the system.

Consequently, all ingredients necessary for the operation of the monopole sources of acoustic and gravitational waves are present in the solar chromosphere. Namely, high level of turbulent fluctuations; partially ionized plasma; ion-temperature fluctuations; non-stationary heat fluctuations related to the ionization energy.

In the framework of the ongoing research we intend to study the efficiency of quadrupole, dipole and monopole sources of acoustic and gravity waves in chromospheric partially ionized turbulent plasma using Lighthill's acoustic analogy and taking into account the effects of stratification, temperature fluctuations and partial ionization in solar atmosphere. Detailed analysis of main characteristics and estimates of total emissivities of acoustic and gravity waves will be done. We will analyze the possible role of acoustic and gravity waves generated by heat fluctuations related to the partial ionization of Solar atmosphere in the both chromospheric and coronal heating in the Sun and other cool stars of solar type that have a partially ionized chromosphere.

4.3 Discussion and summary

Possible chromospheric heating mechanisms have been reviewed in this section. It has been emphasized that the physical processes responsible for chromospheric heating is a major puzzle of solar physics since it was discovered from the observations of line and continuum emissions by non-active solar surface that the temperature in the solar chromosphere (around 6000-7000 K) is much higher than that can be expected for a plasma in radiative equilibrium.

Neither of the proposed mechanisms can account for amount of the energy needed for the heating of the whole chromosphere. Even though these mechanisms can provide considerable contribution in chromospheric heating process, they cannot be the main source of chromospheric heating.

Two complementary approaches, semiempirical and theoretical, that are used for understanding the solar and stellar atmospheres, have been introduced. Empirically derived parameters of Solar atmosphere from one-dimensional model of the solar atmosphere (called SRPM 306) of the quiet-Sun chromosphere have been shown.

Solar atmosphere is significantly superadiabatic and possess ionization zones. The ionization degree depends on the temperature, which steeply rises from lower chromosphere to the chromospheric plateau. Thus the ionization degree is quite high ($10^{-2}-10^{-4}$) in the upper chromosphere and all ingredients necessary for the operation of the monopole sources of acoustic and gravitational waves (high level of turbulent fluctuations; partially ionized plasma; ion-temperature fluctuations; non-stationary heat fluctuations related to the ionization energy) present in the solar chromosphere. The efficiency of quadrupole, dipole and monopole sources of acoustic and gravity waves in chromospheric partially ionized turbulent plasma need to be examined using Lighthill's acoustic analogy.

This novel mechanism of acoustic wave generation by turbulence related to the non-stationary heat sources applied to the study of physical processes in the solar chromosphere is under way presently. We intend to perform detailed analysis of main characteristics and estimates of total emissivities of acoustic and gravity waves. We will analyze the possible role of acoustic and gravity waves generated by heat fluctuations related to the partial ionization of Solar atmosphere in the both chromospheric and coronal heating in the Sun and other cool stars of solar type that have a partially ionized chromosphere.

5 Conclusions

Eventually some conclusions can be drawn. The aim of the thesis is to develop a novel theory of sound generation mechanism by non-stationary heat sources in saturated turbulent flow. The obtained results are applied to infrasound generation in strong convective storms to explain main characteristics of generated infrasound and observed high correlation between infrasound intensity and tornado formation.

The aim of the ongoing research is application of this theory to the study of wave generation processes is partially ionized Solar chromosphere and examination of there role in the chromospheric heating in the Sun and solar type stars that have a partially ionized chromosphere.

The following new results are obtained in the thesis:

- Acoustic wave generation by turbulence in a stratified, moist atmosphere is studied in the framework of a generalized acoustic analogy. It is shown that in saturated moist air turbulence in addition to the Lighthill's quadrupole and dipole sources of sound (related to stratification and temperature fluctuations), there exist monopole sources related to heat and mass production during the condensation of moisture.

- The acoustic power of these monopole sources is determined and it is shown that this radiation is dominant for typical parameters of strong convective storms. The results are in good qualitative agreement with the main observed characteristics of infrasound radiation by strong convective storms, e.g. total acoustic power and characteristic frequency.

- It is estimated that the total power of the source related to moisture is of order 10^7 watts, in qualitative agreement with observations of strong convective storms.

- It is shown that for typical parameters of strong convective storms the peak frequency of infrasound radiation is $\nu_{peak} \approx 0.8$ Hz, which is in a good agreement with observations.

- Detailed spectral analysis of a monopole source of sound related to the heat production during the condensation of moisture are performed.

- A quantitative explanation of the correlation between intensity of infrasound generated by supercell storms and later tornado formation is given. It is shown that low lifting condensation level (LCL) and high values of convective available potential energy (CAPE), which are known to favor significant tornadoes, also lead to a strong enhancement of supercells low frequency acoustic radiation.

- We also believe that this novel mechanism of wave generation by turbulence related to the non-stationary heat sources, when applied to the ionization energy of partially ionized solar atmosphere, will give new results in solar physics and help in understanding of physical processes in the solar chromosphere.

Acknowledgments

I would like to express a big gratitude to my supervisor Prof. George Machabeli for his great help in working.

I am grateful to all co-authors of my papers: Prof. Grigol Gogoberidze from Center of Theoretical Astrophysics, Ilia State University, Georgia and Center or Plasma Astrophysics, K.U.Leuven, Belgium and Philip Morrison from the University of Texas at Austin.

I also appreciate helpful discussions with my colleagues from Center of Theoretical Astrophysics, Ilia State University, Georgia Profs. Zaza Osmanov and Andria Rogava, Drs. Nino Chkheidze, Giorgi Dalakishvili, David Khechinashvili, Irakli Nanobasvili and David Shapakidze.

References

Abdullah A. J. 1966. The "musical" sound emitted by a tornado. *Mon. Wea. Rev.*, 94, 213.

Akhalkatsi M. and Machabeli G.Z. 2000. Generation of electromagnetic waves in the electron-positron plasma in the vicinity of pulsar. *Astrophysics*, 43, 282.

Akhalkatsi M. and Gogoberidze G. 2009. Infrasound generation by tornadic supercell storms. *Quart. J. Roy. Meteor. Soc.*, 135, 935.

Akhalkatsi M. and Gogoberidze G. 2011. Spectrum of infrasound radiation from supercell storms. Accepted for publication to *Quart. J. Roy. Meteor. Soc.*, 137, 229.

Akhalkatsi M. and Gogoberidze G. 2011. *Infrasound generation by turbulent convection.* Chapter of the book: Sound waves: propagation, frequencies and effects (Nova Publishers). (In preparation. Offer to write a chapter was made by publisher on 01.10.2010 and accepted on 30.10.2010. The chapter will be submited till 10.03.2011 and will be published no later than 01.06.2011).

Akhalkatsi M. and Gogoberidze G. 2011. Wave generation in partially ionized Solar chromosphere. In preparation

Akhalkatsi M. and Gogoberidze G. and Morrison P.J. 2004. Infrasound generation by turbulent convection. Eprint arXiv: astro-ph/0409369.

Aschwanden M.J., Tarbell T.D., Nightingale R.W., Schrijver C.J. and Title A. 2000. Time Variability of the "Quiet" Sun Observed with TRACE. II. Physical Parameters, Temperature Evolution, and Energetics of Extreme-Ultraviolet Nanoflares. *The Astrophysical Journal*, 535, 1047.

Bastin F., Lafon P. and Candel S. 1995. Computation of jet mixing noise due to coherent structures: the plane jet case. *J. Fluid Mech.*, 11, 1.

Batchelor G.K. 1967. *An Introduction to Fluid Dynamics.* Cambridge Univ. Press, Cambridge, UK.

Beasley W.H., Georges T.M. and Evans M.W. 1976. Infrasound from convective storms: An experimental test of electrical source mechanisms. *J. Geophys. Res.*, 81, 3133.

Bedard A.J. 1998. Infrasonic detection of severe waether. *J.Proc. 19th Conf. Severe Storms, 14-18 Sept. 1998, Minneapolis, Minn..*

Bedard A.J. and Georges T.M. 2000. Atmospheric infrasound. *Phys. Today*, 53, 32.

Bedard A.J., Bartram B.W., Keane A.N., Welsh D.C. and Nishiyama R.T. 2004a. The Infrasound Network (ISNet): Background, Design Details and Display Capability as an 88D Adjunct Tornado Detection Tool. *Proceedings of 22nd Conference on Severe Local Storms, Boston, MA, USA, 4-8 October.*

Bedard A.J., Bartram B.W., Entwistle B., Golden J., Hodanish S., Jones R.M., Nishiyama R.T., Keane A.N., Mooney L., Nicholls M., Szoke E.J., Thaler E. and Welsh D.C. 2004b. Overview of the ISNet Data Set and Conclusions and Recommendations from a March 2004 Workshop to Review ISNet Data. *Proceedings of 22nd Conference on Severe Local Storms, Boston, MA, USA, 4-8 October.*

Bedard A.J. 2005. Low-Frequency Atmospheric Acoustic Energy Assiciated with Vortices Produced by Thunderstorms. *Monthly Weather Review*, 133, 241.

Biermann L. 1946. *Naturwissenschaften*, 33, 118.

Bluestein H.B. 1992. *Synoptic-Dynamic Meteorology in Midlatitudes.* Oxford University Press, Vol. 1, 448.

Bolton D. 1980. The Computation of Equivalent Potential Temperature. *Mon. Wea. Rev.*, 108, 1046.

Bowman H.S. and Bedard A.J. 1971. Observations of infrasound and subsonic disturbances related to severe weather. *Geophys. J. R. Astr. Soc.*, 26, 215.

Buneman O. 1963. Excitation of field aligned sound waves by electron streams. *Phys. Rev. Lett.*, 10, 285.

Carlsson M. 2007. Modeling the Solar Chromosphere, *in The Physics of Chromospheric Plasmas, Ed. Heinzel P., Dorotovic I. and Rutten R. J., ASP Conf. Ser.*, 368, 49.

Carlsson M. and Stein R.F. 1992. Non-LTE radiating acoustic shocks and CA II K2V bright points. *Astrophysical Journal*, 397, L59.

Christensen-Dalsgaard J. 1980. On adiabatic non-radial oscillations with moderate or large L. *Royal Astronomical Society, Monthly Notices*, 190, 765.

Christensen-Dalsgaard J. and Gough D.O. 1980. Is the Sun helium-deficient. *Nature*, 288, 544.

Colgate S.A. and McKee C. 1969. Elecctrostatic sound in clouds and lightning. *J. Geophys. Res.*, 74, 5379.

Colonius T., Lele S.K. and Moin P. 1994. The scattering of sound waves by a vortex: numerical simulations and analytical solutions. *J. Fluid Mech.*, 206, 271.

Colonius T., Moin P. and Lele S.K. 1995. Direct computation of aerodynamic sound. *Report TF-66 Thermosciences Division, Department of Mech. Engineering, Stanford University*.

Crighton D.G. and Huerre P. 1990. Shear-layer pressure fluctuations and superdirective acoustic sources. *J. Fluid Mech.*, 220, 355.

Curle N. 1955. The Influence of Solid Boundaries on Aerodynamic Sound. *Proc. Roy. Soc. London, GB*, 231A, 1187, 505.

Davies-Jones R.P. 1993. Helicity trends in tornado outbreaks. *Preprints of 17th Conf. on Severe Local Storms, St. Louis, MO, Amer. Meteor. Soc.*, 56.

Debussche A., Dubois T. and Teman R. 1993. The nonlinear Galerkin method: A multi-scale method applied to the simulation of homogeneous turbulent flows. *ICASE Report*, 93, 93.

Erdelyi R. and James S.P. 2004. Can ion-neutral damping help to form spicules? II. Random driver. *Astronomy and Astrophysics*, 427, 1055.

Farley D.T. 1963. Theory of equatorial electrojet plasma waves: new developments and current status. *J. Atmos. Terr. Phys.*, 68, 6083.

Ffowcs Williams J.E. and Hall L.H. 1970. Aerodynamic Sound Generation by Turbulent Flow in the Vicinity of a Scattering Half Plane. *J. Fluid Mech.*, 40, 657.

Freund J.B. 1999. acoustic Sources in A Turbulent Jet: A Direct Numerical Simulation Study. *AIAA Pap.*, 99, 1858.

Fontenla J.M., Avrett E.H. and Loeser R. 1991. Energy balance in the solar transition region. II - Effects of pressure and energy input on hydrostatic models. *The Astrophysical Journal*, 377, 712.

Fontenla J.M., Avrett E.H. and Loeser R. 1993. Energy balance in the solar transition region. III - Helium emission in hydrostatic, constant-abundance models with diffusion. *The Astrophysical Journal*, 406, 319.

Fontenla J.M., White O.R., Fox P.A., Avrett E.H. and Kurucz R.L. 1999. Calculation of Solar Irradiances. I. Synthesis of the Solar Spectrum. *The Astrophysical Journal*, 518, 480.

Fontenla J.M. 2005. Chromospheric plasma and the Farley-Buneman instability in solar magnetic regions. *Astronomy and Astrophysics*, 442, 1099.

Fontenla J.M., Balasubramaniam K.S. and Harder J. 2007. Semiempirical Models of the Solar Atmosphere. II. The Quiet-Sun Low Chromosphere at Moderate Resolution. *The Astrophysical Journal*, 667, 1243.

Fontenla J.M., Peterson W.K. and Harder J. 2008. Chromospheric heating by the Farley-Buneman instability. *Astronomy and Astrophysics*, 480, 839.

Fossum A. and Carlson M. 2005. High-frequency acoustic waves are not sufficient to heat the solar chromosphere. *Nature*, 435, 919.

Freund J.B. 2003. Noise-source turbulence statistics and the noise from a Mach 0.9 jet. *Phys. Fluids*, 15, 1788.

Georges T.M. 1973. Infrasound from Convective Storms: Examining the Evidence. *Reviews of Geophysics and Space Physics*, 11, 571.

Georges T.M. and Greene G.E. 1975. Infrasound from Convective Storms. Part IV. Is It Useful for Storm Warning? *J. Appl. Met.*, 17, 1303.

Georges T.M. 1976. Infrasound from convective storms. Part II: A critique of source candidates. NOAA Tech. Rep. ERL 380WPL, 49, 59.

Georges T.M. 1988 in *Instruments and Techniques for Thunderstorm Observation and Analysis*. University of Oklahoma Press (editor E. Kessler), 75.

Gingerich O. and de Jager C. 1968. The Bilderberg model of the photosphere and low chromosphere. *Sol. Phys.*, 3, 5.

Gingerich O., Noyes R.W., Kalkofen W. and Cuny Y. 1971. *Sol. Phys.*, 18, 347.

Gogoberidze G., Kahniashvili T. and Kosowsky A. 2007. Spectrum of gravitational radiation from primordial turbulence *Phys. Rev. D*, 76, 083002.

Gogoberidze G., Voitenko Y., Poedts S. and Goossens M. 2009. Farley-Buneman Instability in the Solar Chromosphere. *The Astrophysical Journal Letters*, 706, L12.

Goldreich P. and Kumar P. 1990. Wave generation by turbulent convection. *Astrophysical Journal*, 363, 694.

Goldstein M.E. 1976. *Aeroacoustics*. McGraw Hill, New York.

Goldstein M.E. 1984. Aeroacoustics of turbulent shear flows. *Ann. Rev. Fluid Mech.*, 16, 263.

Goldstein M.E. 2002. A generalized acoustic analogy. *J. Fluid Mech.*, 488, 315.

Goodman M.L. 2004. On the creation of the chromospheres of solar type stars. *Astronomy and Astrophysics*, 424, 691.

Gossard E.E. and Hooke W.H. 1975. *Waves in the atmosphere: Atmospheric infrasound and gravity waves - Their generation and propagation.* Elsevier, New York.

Gutin L. 1948. On the Sound Field of a Rotating Propeller. *NACA TM*, 1195.

Hasan S.S. and van Ballegooijen A.A. 2008. Dynamics of the Solar Magnetic Network. II. Heating the Magnetized Chromosphere. *The Astrophysical Journal*, 680, 1542.

Hinze J.O. 1975. *Turbulence*. McGraw Hill, New York, 244.

Howe M.S. 1977. Sound generation by a turbulent dipole. *J. Sound and Vibration*, 51, 451.

Howe M.S. 2001. in *Sound-flow interactions* (editors Y.Auregan, A.Maurel, V.Pagneux and J.F.Pinton), Springer-Verlag, Berlin, 31.

Kato S. 1966. The Response of an Unbounded Atmosphere to Point Disturbances. I. Time-Harmonic Disturbances. *Astroph.J.*, 143.

Kraichnan R.H. 1964. Decay of isotropic turbulence in the Direct Interaction Approximation. *Physics of Fluids*, 7, 1163.

Kumar P. and Goldreich P. 1989. Nonlinear interactions among solar acoustic modes. *Astrophysical Journal*, 342, 558.

Lamb H. 1945. *Hydrodynamics*. Dover, New York.

Lemon L.R. and Doswell III C.A. 1979. Severe thunderstorm evolution and mesocyclone structure as related to tornadogenesis. *Mon. Wea. Rev.*, 107, 1184.

Libbrecht K.G. 1988. The excitation and damping of solar oscillations. *In ESA, Seismology of the Sun and Sun-Like Stars*, p.3.

Lighthill M.J. 1952. On Sound Generated Aerodynamically. I. General Theory. *Proc. R. Soc. London Ser.* A, 211, 564.

Lighthill M.J. 1954. On Sound Generated Aerodynamically. II. Turbulence as a source of sound. *Proc. R. Soc. London Ser.* A, 222, 1.

Lilley G.M. 1974. On the noise from jets. Noise Mechanism. *AGARD-CP*, 131, 13.1.

Lilley G.M. 1994. The radiated noise from isotropic turbulence. *Theor. Comput. Fluid Dyn.*, 6, 281.

Liperovsky V.A., Meister C.V., Liperovskaya E.V., Popov K.V. and Senchenkov S.A. 2000. On the generation of modified low-frequency Farley-Buneman waves in the solar atmosphere. *Astronomische Nachrichten*, 321, 129.

Markowski P.M., Straka J.M., Rasmussen E.N. and Blanchard D.O. 1998. Variability of storm-relative helicity during VORTEX. *Mon. Wea. Rev.*, 126, 2959.

Markowski P.M., Straka J.M. and Rasmussen E.N. 2002. Direct surface thermodynamic observations within the rear-flank downdrafts of nontornadic and tornadic supercells. *Mon. Weather Rev.*, 130, 1692.

Markowski P.M., Straka J.M. and Rasmussen E.N. 2003. Tornadogenesis resulting from the transport of circulation by a downdraft. *J. Atmos. Sci.*, 60, 795.

Markowski P.M. and Richardson Y.P. 2009. Tornadogenesis: Our current understanding, forecasting considerations, and questions to guide future research. *J. Atmos. Res.*, 93, 3.

McCaul E.W. 1991. Buoyancy and shear characteristics of hurricane tornado environments. *Mon. Wea. Rev.*, 119, 1954.

McCaul E.W. and Weisman M.L. 1996. Simulations of shallow supercell storms in landfalling hurricane environments. *Mon. Wea. Rev.*, 124, 408.

Mitchell B.E., Lele S.K. and Moin P. 1992. Direct computation of sound from a compressible co-rotating vortex pair. *AIAA Pap.*, 92, 0374.

Mitchell B.E., Lele S.K. and Moin P. 1995. Direct computation of the sound generated by subsonic and supersonic axisymmetric jets. *Report TF-66 Thermosciences Division, Department of Mech. Engineering, Stanford University.*

Monin A.S. and Yaglom A.M. 1975. *Statistical Fluid Mechanics.* MIT Press.

Naugolnykh K. and Rybak S. 2008. Infrasound induced instability by modulation of condensation process in the atmosphere. *Acoust. Soc. Amer. J.*, 124, 1.

Nicholls M.E. and Pielke R.A. 1994. Thermal compression waves. I: Total energy transfer. *Quart. J. Roy. Meteor. Soc.*, 120, 305.

Nicholls M.E. and Pielke R.A. 1994. Thermal compression waves. II: Mass

adjustment and vertical transfer of total energy. *Quart. J. Roy. Meteor. Soc.*, 120, 333.

Nicholls M.E. and Pielke R.A. 2000. Thermally-induced compression waves and gravity waves generated by convective storms. *J. Atmos. Sci.*, 57, 3251.

Nicholls M.E., Pielke Sr.R.A. and Bedard A. 2004. Preliminary Numerical Simulations of Infrasound Generation Processes by Severe Weather Using a Fully Compressible Numerical Model. *Proceedings of 22nd Conference on Severe Local Storms, Boston, MA, USA, 4-8 October.*

Noble J.M. and Tenney S.M. 2003. Observations of severe storms with infrasound. *Acoust. Soc. Amer. J.*, 114, 2367.

Ostashev V.E., Georges T.M., Clifford S.F. and Goedecke G.H. 2001. Acoustic sounding of wind velocity profiles in a stratified moving atmosphere. *Acoust. Soc. Amer. J.*, 109, 2682.

Panickar P., Srinivasan K., Raman G. and Juve D. 2005. Nonlinear interactions as precursors to mode jumps in resonant acoustics. *Phys. Fluids*, 17, 096103.

Parker E.N. 1988. Nanoflares and the solar X-ray corona. *Astrophysical Journal*, 330, 474.

Phillips O.M. 1960. On the generation of sound by supersonic turbulent shear layers. *J. Fluid Mech.*, 9, 1.

Pielke R.A, Nicholls M.E. and Bedard A.J. 1993. Use of thermal compression waves to assess latent heating from clouds. *Eos*, 74, 493.

Powell A. 1960. Aerodynamic Noise and the Plane Boundary *J. Acoust. Soc. Am.*, 32, 8, 982.

Proudman I. 1952. *The generation of noise by isotropic turbulence.* Proc. R. Soc. London Ser. A, 214, 119.

Rabin D. and Moore R. 1984. Heating the Sun's lower transition region with fine-scale electric currents. *Astrophysical Journal*, 285, 359.

Rasmussen E.N. and Blanchard D.O. 1998. A Baseline Climatology of Sounding-Derived Supercell and Tornado Forecast Parameters. *Weather and Forecasting*, 13, 4, 1148.

Rasmussen E.N. 2003. Refined Supercell and Tornado Forecast Parameters. *Weather and Forecasting*, 18, 3, 530.

Rotunno R. and Klemp J.B. 1982. The influence of the shearinduced pressure gradient on thunderstorm motion. *Mon. Wea. Rev.*, 110, 136.

Sarkar S. and Hussaini M.Y. 1993. Computation of the sound generated by isotropic turbulence. *ICASE Report*, 93, 74.

Schecter D.A., Nicholls M.E., Persing J., Bedard A.J. and Pielke Sr. R.A. 2008. Infrasound emitted by tornado-like vortices: Basic theory and a numerical comparison to the acoustic radiation of a single-cell thunderstorm. *J. Atmos. Sci.*, 65, 3, 685.

Schwarzschild M. 1948. On Noise Arising from the Solar Granulation. *Astrophysical Journal*, 107, 1.

Seror C., Sagaut P., Bailly C. and Juve D. 2001. On the radiated noise computed by large-eddy simulation. *Phys. Fluids*, 13, 476.

Socas-Navarro H. 2007. Semiempirical Models of Solar Magnetic Structures. *The Astrophysical Journal Supplement Series*, 169, 439.

Stein R.F. 1967. Generation of Acoustic and Gravity Waves by Turbulence in an Isothermal Stratified Atmosphere. *Sol. Phys.*, 2, 385.

Sturrock P.A. 1999. Chromospheric Magnetic Reconnection and Its Possible Relationship to Coronal Heating. *The Astrophysical Journal*, 521, 451.

Szoke E.J., Bedard A.J., Thaler E. and Glancy R. 2004. A comparison of inset data with radar data for tornadic and potentially tornadic storms in northeast colorado. *Proceedings of 22nd Conference on Severe Local Storms, Boston, MA, USA, 4-8 October.*

Thompson R.L. and Edwards R. 2000. An Overview of Environmental Conditions and Forecast Implications of the 3 May 1999 Tornado Outbreak. *Weather and Forecasting*, 15, 6, 682.

Thompson R.L., Edwards R., Hart J.A., Elmore K.L. and Markowski P.M. 2003. Close proximity soundings within supercell environments obtained from the Rapid Update Cycle. *Weather Forecast*, 18, 1243.

Vernazza J.E., Avrett E.H. and Loeser R. 1981. Structure of the solar chromosphere. III - Models of the EUV brightness components of the quiet-Sun. *Astrophysical Journal Supplement Series*, 45, 635.

Weisman M. L. and Klemp J. B. 1982. The dependence of numerically simulated convective storms on vertical wind shear and buoyancy. *Mon. Wea. Rev.*, 110, 504.

Whitmire J. and Sarkar S. 2000. Validation of acoustic-analogy predictions for sound radiated by turbulence. *Phys. Fluids*, 12, 381.

Witkowska A., Brasseur J.G. and Juve D. 1995. Numerical study of noise from stationary isotropic turbulence. *AIAA Pap*, 95, 037.